Synthesis of Oligothiophene-Bridged Bisporphyrins and Study of the Linkage Dependence of the Electronic Coupling

Fabrice Odobel,*[a] S. Suresh,[a] Errol Blart,[a] Yohann Nicolas,[a] Jean-Paul Quintard,[a] Pascal Janvier,[a] Jean-Yves Le Questel,[b] Bertrand Illien,[b] David Rondeau,[c] Pascal Richomme,[c] Tilmann Häupl,[d] Staffan Wallin,[d] and Leif Hammarström[d]

Dedicated to Dr. Jean Villieras on the occasion of his 62nd birthday

Abstract: A set of twelve porphyrin dimers has been prepared to give information on how the type of connectivity between a porphyrin core and a bridge can influence the interporphyrin electronic interaction. The new porphyrin systems are substituted directly at the *meso* position with an oligothiophene chain tethered either with a single C–C sigma bond, a *trans* ethylenyl group, or a acetylenyl group. The compounds are easily obtained by palladium-catalyzed cross-coupling reactions (Stille, Heck, and Sonogashira) between 5-iodo-10,15,20-(3,5-di*tert*-butylphenyl)porphyrin and the appropriate oligothiophene derivative. This synthetic approach is straightforward and very effective for preparing oligothiophene-based porphyrin systems. The absorption spectra and the fluorescence properties of the dimers demonstrated the crucial importance of the characteristics of the chemical bond used to connect the bridge to the porphyrin unit. The magnitude of the electronic communication can thus be significantly modulated by altering the type of bond connectivity used to link the chromophore to the bridge. The present work shows that an oligothiophene spacer is a viable class of linker for connecting porphyrins, and that a quaterthiophene appended with ethynyl linkages affords a high electronic interaction over a distance as large as 28 Å. A detailed computational study of these dimers has clarified the conditions needed for a conjugated system to behave as a molecular wire. These conditions are full planarity of the molecule and proper energy matching between the frontier orbitals of the bridge and the porphyrin. Intermolecular energy transfer in asymmetrical dyads composed of a zinc porphyrin and a free-base porphyrin has been studied by fluorescence spectroscopy. In all systems, this process is more than 98% efficient, and its rate constant decreases steadily in the order **4ZH** > **1ZH** > **3ZH** ≈ **2ZH**. Thus, the largest rate ($k_{EnT} = 1.2 \times 10^{11}\,s^{-1}$) was found in the dyad linked with bisethynyl quaterthiophene, which represents the longest bridge within the series. These results clearly demonstrate that strong communication and also efficient photoinduced processes can be promoted over a large distance if the electronic structure of the molecular connector is appropriately chosen.

Keywords: computer chemistry · energy transfer · fluorescence spectroscopy · molecular devices · porphyrinoids

[a] Dr. F. Odobel, Dr. S. Suresh, Dr. E. Blart, Y. Nicolas, Prof. J.-P. Quintard, Dr. P. Janvier
Laboratoire de Synthèse Organique, UMR 6513 CNRS
Faculté des Sciences et des Techniques de Nantes, B.P. 92208
2, rue de la Houssinière, 44322 Nantes Cedex 3 (France)
Fax: (+33) 2-51-12-54-02
E-mail: odobel@chimie.univ-nantes.fr

[b] Dr. J.-Y. Le Questel, Dr. B. Illien
Laboratoire de Spectrochimie
Faculté des Sciences et des Techniques de Nantes, B.P. 92208
2, rue de la Houssinière, 44322 Nantes Cedex 3 (France)

[c] Dr. D. Rondeau, Dr. P. Richomme
Laboratoire de Spectrométrie de Masse, Faculté des Sciences
2, boulevard Lavoisier, 49045 Angers Cedex (France)

[d] Dr. T. Häupl, S. Wallin, Dr. L. Hammarström
Department of Physical Chemistry, Uppsala University
Box 532, 751 21 Uppsala (Sweden)

Introduction

The control of electronic interactions in bridged multicomponent systems is a crucial factor for the rational design of photonic molecular devices. It is particularly important for the development of devices featuring a cascade of electron- or energy-transfer steps to achieve efficient excited-state energy transport or long-lived charge-separated states.[1, 2] Furthermore, electronic communication is also an important property for the design of optoelectronic devices[3, 4] and mixed-valence compounds.[5] In this context, the importance of the linkage is quite significant because it has two fundamental roles. First, a rigid spacer positions two neighboring active centers at a fixed distance and with a well-defined geometry. Second, the spacer provides a way to promote electronic communication, and

  0947-6539/02/0813-3027 $ 20.00+.50/0

therefore facilitates electron and/or energy migration between the two bridged units.

Electronic coupling can come either by through-space or through-bond interactions, and both types of interaction can coexist in some systems. According to current theory, the electronic coupling in a donor–acceptor bridged system (DABS) is usually dominated by through-bond interactions, across the electronic structure of the bridge, and is known to decrease exponentially with the separation distance (d) between A and D [Eq. (1)].[6]

$$H_{AD} = H^{\circ}_{AD} \exp\left(-\frac{\beta}{2}(d - d^{\circ})\right) \quad (1)$$

Abstract in French:
Une série de douze molécules bis-porphyrines a été synthétisée afin d'étudier l'influence du mode de connectivité sur l'interaction électronique inter-porphyrine. Ces nouveaux systèmes bis-porphyrines sont directement substitués en position méso par une chaîne oligothiophène liée soit par une simple liaison C–C, soit par un groupe trans éthènyle, soit par un groupe éthynyle. Ces composés sont facilement synthétisés par une réaction de couplage croisé catalysée par le palladium (Stille, Heck, Sonogashira) entre la 5-iodo-10,15,20-(3,5-ditert-butylphényl) porphyrine et le dérivé oligothiophène approprié. Cette approche synthétique est directe et particulièrement efficace pour la préparation de tels systèmes porphyriniques. Les spectres d'absorption et de fluorescence montrent l'importance cruciale de la nature de la liaison entre le connecteur et la porphyrine. L'amplitude de la communication électronique peut ainsi être modulée de façon notable en modifiant le type de connectivité entre le chromophore et le pont. Ce travail démontre que les oligothiophènes sont une famille de molécules appropriées pour relier des porphyrines et que l'espaceur quaterthiophène relié par des groupes éthynyles permet une interaction électronique importante jusqu'à une distance de l'ordre de 28 Å. Une étude de modélisation moléculaire par une méthode semi-empirique a précisé les caractéristiques structurales et électroniques requises pour qu'un système conjugué permette d'assurer un couplage électronique optimal. Ces caractéristiques sont respectivement la planéité du système et une bonne proximité énergétique entre les orbitales frontières du connecteur et celles de la porphyrine. Le transfert d'énergie intermoléculaire dans des dyades asymétriques, composées d'une porphyrine de zinc et d'une porphyrine base libre, a été étudié par spectroscopie de fluorescence. Dans tous les systèmes, l'efficacité du transfert d'énergie photoinduit est supérieure à 98 % et sa vitesse décroît dans l'ordre suivant: ***4 ZH > 1 ZH > 3 ZH ≈ 2 ZH****. Ainsi, la constante de vitesse la plus élevée ($k_{EnT} = 1.2 \times 10^{11}\,s^{-1}$) est observée avec la dyade possédant l'espaceur diéthynyl-quaterthiophène qui représente le plus long connecteur dans la série de molécules étudiées. Ces résultats démontrent clairement qu'une bonne communication électronique ainsi qu'une grande efficacité des processus photoinduits peuvent être envisagées sur de longues distances si la structure de l'espaceur est convenablement choisie.*

H°_{AD} is the electronic coupling when donor and acceptor are at a center-to-center distance d° and β is the attenuation or damping factor that characterizes the bridge and the DA pair. In such a model, the electronic coupling arises from the overlap of the frontier orbitals of the donor and the acceptor with those of the bridge, and depends on their respective energy proximity.[1, 3] Highly conjugated organic bridges[7, 8] mediate small β values ranging from $0.1-0.6\ \text{Å}^{-1}$, whereas saturated spacers,[9] such as cyclohexane and norbornane, are characterized by β values around $0.8-1\ \text{Å}^{-1}$.

The importance of electronic interactions on electron-transfer rates has been examined both in synthetic and natural systems, and extensive theoretical analysis has been devoted to modeling this property.[6–10] For example, strong to weak electronic couplings are found in biological macromolecules such as proteins.[9, 11] It is now well-accepted that hydrogen bonds inside proteins can play a crucial role in establishing a pathway that mediates electronic coupling between donors and acceptors embedded in such media.[12, 13] One of the most relevant example of electronic coupling in biological systems is undoubtedly found in light harvesting antennae and in the reaction center during the photochemical processes of photosynthesis.[14] In this area, numerous elegant studies with covalently linked dyads including works of Paddon-Row,[15, 16] Moore,[17] Sauvage,[18] Osuka,[19] Therien,[20, 21] and others[1, 9, 11–13, 22] have shown compelling evidence of the crucial role of bridge-mediated electronic coupling on the rate of the photoinduced charge separation. More recently, Wasielewski and co-workers[7, 23] have developed a very interesting DBAS linked by a series of *para*-phenylene vinylene oligomers of various lengths. These molecular systems exhibit very weak dependence of photoinduced electron transfer thanks to hopping and tunneling modes mediated by the bridge ($\beta = 0.04\ \text{Å}^{-1}$).

Coming back to Equation (1), it can be inferred that through-space interactions display very strong distance dependence ($\beta = 2\ \text{Å}^{-1}$ in a vacuum)[3] and are negligible above 5 Å. Thus electronic communication over long distances can be considered to be purely through-bond interactions across a connector. Through-bond interactions hold a particular interest, in that electronic coupling can be favorable over long distance if the bridge has a small β value.

The development of appropriate spacers that promote high electronic interactions is an important issue from the viewpoint of maintaining a high rate of energy and/or electron transfer whilst increasing the distance between donor and acceptor. Indeed charge separation[1–4, 6–8, 24] or photoinduced energy transfer following Dexter's mechanism[25] are two processes that are highly sensitive to the magnitude of the electronic coupling. Therefore, strong electronic coupling will facilitate intramolecular energy and electron transfers. Hence, a promising way to achieve long-range electron and energy transfers with few molecular active units is to separate them by long, rigid spacers that promote small values of the β attenuation factor.

For the reasons stated above, we started a program aimed at designing bridged, electronically coupled porphyrins to investigate the benefits of electronic coupling for intramolecular energy and electron migration over long distances.

  0947-6539/02/0813-3028 $ 20.00+.50/0 *Chem. Eur. J.* **2002**, *8*, No. 13

We chose porphyrin as the molecular component for this purpose because its versatile photo- and electrochemical properties make it possible to use porphyrin either as a light collector, an electron donor, or an electron acceptor depending on the nature of the metal ions complexed inside the macrocycle and/or its peripheral substituents.[26, 27]

Until recently, porphyrin arrays designed for photoinduced energy and electron transfers, generally featured very weak electronic interactions, mostly because the bridge linking the chromophores was appended to the *meso*-aryl substituents of the porphyrin.[17–19, 24, 28, 29] In that case, the electronic communication was suppressed because, in *meso*-tetraaryl porphyrins, the aromatic substituent is forced out of the porphyrin macrocycle, thus interrupting the conjugation with this substituent.[30] Pioneering works by Arnold[31] and Anderson[32] followed by those of Therien[20, 21] and other groups[33] demonstrated that an oligoynyl bridge provides exceptional interporphyrin electronic communication if connected directly to the *meso* position of the porphyrin macrocycle.

In the last decade, the search for molecular wires to mediate long-distance interactions has driven an upsurge in the amount of research and development of molecular electronics and for the construction of photonic molecular devices.[34] Among them, π-conjugated spacers are good candidates because their high effective conjugation could result in wire-like behavior due to small β attenuation.

Oligothiophenes are a particularly appealing class of linkers, since they are abundantly used for conducting materials,[35] and their synthetic chemistry has been extensively described in the literature.[36] In addition to their uses as advanced materials for "plastic electronics" these compounds are attractive as π-conjugated oligomers for molecular wires.[34] The weaker resonance energy of thiophene relative to benzene favors longer effective conjugation, which permits long-range electron delocalization. Furthermore, since Arnold and colleagues[37] first reported the utilization of a thiophene unit to connect porphyrins, this class of linker has been used by Effenberger and Port[38] in light-harvesting systems and, more recently, by Higuchi.[39]

In order to identify a suitable connector for large electronic coupling, we investigated several bridging groups in porphyrin dyads. In this paper, we report on the synthesis of bisporphyrin compounds, in which two triaryl porphyrin moieties are connected through an oligothiophene bridge directly tethered at the *meso* position by three different chemical links: a C–C single bond, a *trans* double bond, or a triple bond (Scheme 1). The electronic coupling was shown to be highly dependent on the characteristics of the chemical bond used to attach the oligothiophene unit. UV-visible absorption spectroscopy, fluorimetry, and computational studies were conducted on the twelve bisporphyrin systems **1**–**4** to investigate the degree of electronic interaction in these arrays.

Results and Discussion

Synthesis: There are basically two major approaches for the preparation of multiporphyrins arrays (Scheme 2).

The first strategy (route a), which has been used for a long time, consists of the condensation of an aldehyde with a pyrrole derivative, most generally dipyrrylmeth-

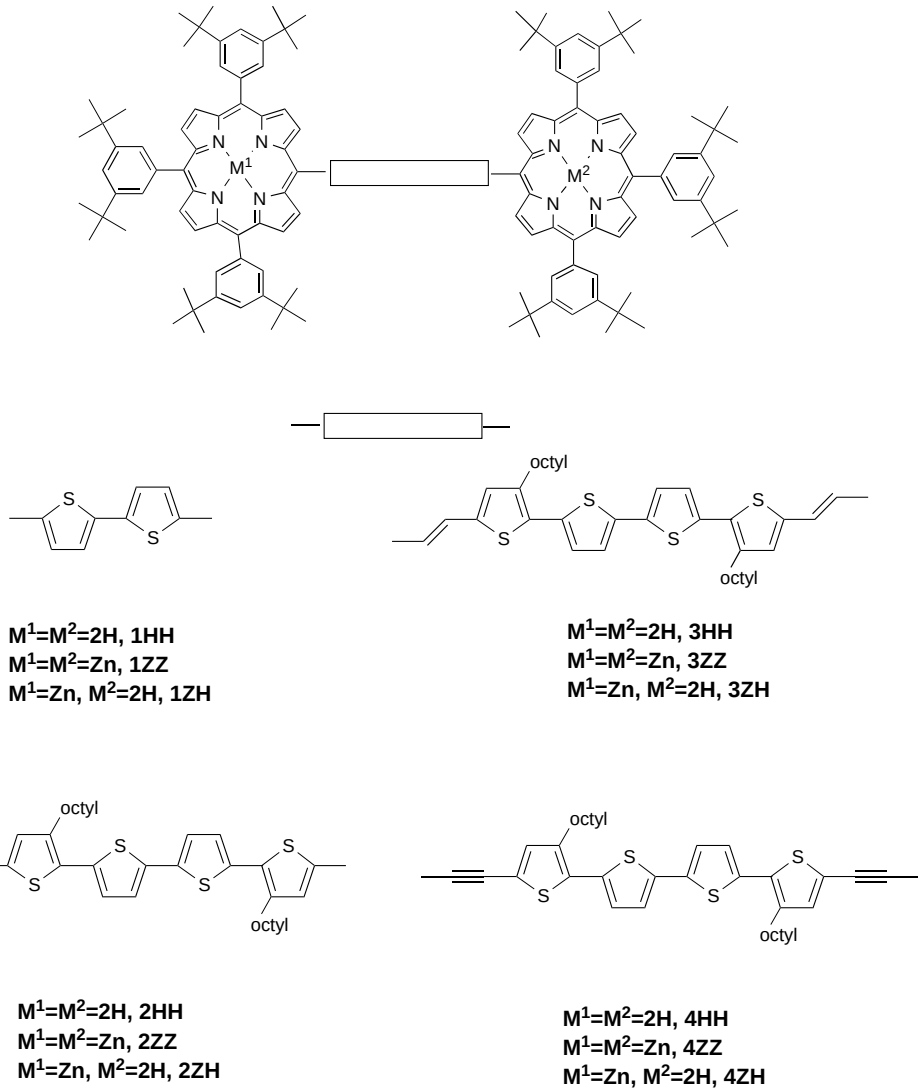

Scheme 1. Dyads studied in this work.

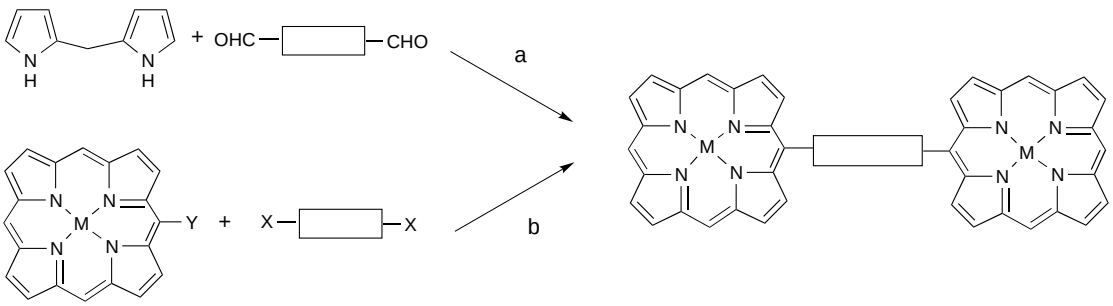

Scheme 2. Two fundamental synthetic strategies for the preparation of bis-porphyrins. X, Y are reactive groups to assemble the spacer to the porphyrin.

ane.[12, 18, 19, 26, 28, 40] With this approach, every porphyrin module is generally constructed all together in the last step of the synthesis. The second approach (route b), developed more recently, is based on the utilization of preformed porphyrin building blocks that are subsequently joined together by palladium cross-coupling reactions with the appropriately functionalized linker.[41] Relevant examples include elegant covalently linked porphyrin arrays synthesized by Lindsey and colleagues.[42] This latter route offers the advantage of a potential stepwise construction of the array, which is highly desirable for the preparation of multiporphyrin systems that contain a wide variety of differently substituted or/and metalated porphyrins. The main difference of these new bisporphyrin systems lies in the direct link of the bridge at the *meso* position of a triaryl porphyrin (Scheme 1). Furthermore, contrary to octaalkyl porphyrins, the porphyrin macrocycle used in this work lacks substituents at the β pyrrole positions, therefore the potential for steric hindrance between the alkyl chains and the spacer is considerably reduced.

The synthetic strategy used for the preparation of the porphyrin dyads **1**–**4** is based on the second strategy, usually named the "building-block approach". This implies the use of two key building blocks: the iodo porphyrin **9**[43, 44] and the quaterthiophene **13**.[45] The synthesis of the porphyrin building block **8** has been improved both in terms of overall yield and speed of purification compared with our previous approach.[43] First, unsubstituted dipyrrylmethane was treated with di*tert*-butylbenzaldehyde to generate the bisaryl porphyrin **6** in good yield (Scheme 3). Then, monobromination of this porphyrin was achieved in cold chloroform by controlling the stoichiometric amount of *N*-bromosuccinimide (NBS) added. The desired porphyrin **7** was separated from unreacted porphyrin **6** by a simple precipitation with petroleum ether. Bromoporphyrin **7** was then subjected to a Suzuki cross-coupling reaction[46] with the known 3,5-di(*tert*-butyl)phenyl boronic acid[47] following the Therien protocol;[48] this afforded the trisaryl porphyrin **8** in 92% yield. Iodination of the free *meso* position of **8** was achieved by using the mixture iodine/iodophenyl bis(trifluoroacetate) in chloroform to give a yield of 90%.[43, 44, 49] At this stage of the synthesis, porphyrin **9** was metalated by zinc in order to avoid palladium insertion during subsequent catalyzed steps.

Quaterthiophene **13** was obtained in 86% yield by Stille coupling between the bis(tributylstannyl) bisthiophene **12** and bromooctylthiophene **11** (Scheme 4). Interestingly, the yield of this reaction dropped to 43% when bis(tributylstannyl)

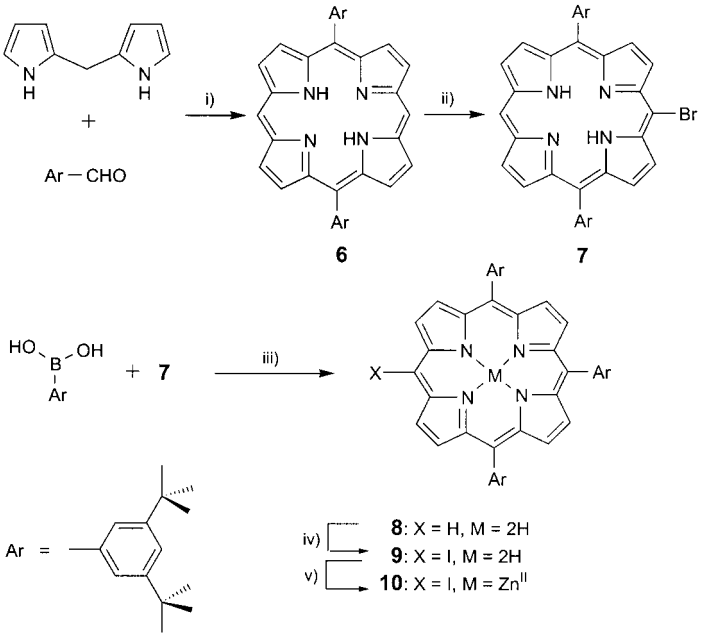

Scheme 3. Synthesis of the key porphyrin building block **9**. i) CH_2Cl_2, TFA then DDQ (73%); ii) 0.8 equiv NBS, 40°C, $CHCl_3$ (65%); iii) $Ba(OH)_2$, $8H_2O$, Pd_2dba_3,$CHCl_3$/PPh_3, DME/H_2O (92%); iv) I_2/$(CF_3CO_2)_2IPh$, $CHCl_3$ (96%); v) $Zn(OAc)_2$, $4H_2O$, $CHCl_3$/CH_3OH, quantitative.

bisthiophene **12** was replaced by bis(trimethylstannyl) bisthiophene. With the latter reagent, the major product formed was 3,3‴″bis(octyl)-2,2′:5′,2″:5″,2‴:5‴,2⁗:5⁗,2⁗′:5⁗′,2⁗″-hexathiophene, arising most probably from homocoupling of the tin bisthiophene before it reacted with **11**. This side reaction has already been reported by several other authors.[50] Quaterthiophene **13** was subjected to a twofold bromination with NBS in chloroform to yield dibromoquaterthiophene **14**, which can undergo subsequent functionalization.

Quaterthiophene **13** was converted in one step into the bis(trismethylstannyl) quaterthiophene **15** by deprotonation with *n*BuLi followed by quenching with trimethyltin chloride. Quaterthiophene **13** was also functionalized with acetylenic groups by treating the dibromo **14** with trimethylsilylacetylene under Sonogashira conditions followed by alkaline desilylation to afford **18**. Bisvinyl quaterthiophene **16** was obtained by Stille coupling between vinyltributyltin and dibromoquaterthiophene **14** in 76% yield.

  0947-6539/02/0813-3030 $ 20.00+.50/0 *Chem. Eur. J.* **2002**, *8*, No. 13

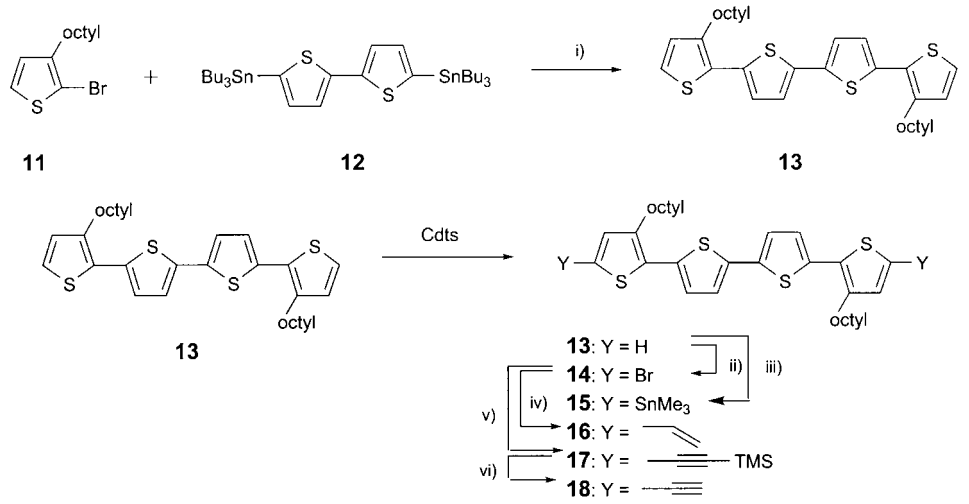

Scheme 4. Synthesis of the quaterthiophene bridges. i) Pd_2dba_3, CH_3Cl/PPh_3, THF/DMF (84%); ii) NBS, $CS_2/CHCl_3$, 0°C (96%); iii) BuLi/THF then Me_3SnCl (55%); iv) $CH_2CHSnMe_3$, $Pd(PPh_3)_4$, DMF (76%); v) Pd_2dba_3, CH_3Cl, PPh_3, TMS/CCH, iPr_2NH, CuI (80%); vi) KOH, MeOH/benzene (72%).

The final step involved a palladium-catalyzed cross-coupling reaction between zinc iodoporphyrin **10** and the appropriate functionalized quaterthiophene. Bisporphyrin **1ZZ** was obtained in 72% yield according to a Stille cross-coupling between **12** and **10** in DMF at 90°C. Similarly, dyad **2ZZ** was prepared in 60% yield by treatment of **10** with the bis(trimethylstannyl) quaterthiophene **15**. The Heck coupling between **10** and **16** was conducted under several catalytic conditions.[51] The standard catalytic system with $Pd(OAc)_2$/trisphenylphosphine did not lead to any detectable trace of dyad **3ZZ**. Replacing the trisphenylphosphine ligand by tris(*o*-tolyl)phosphine, as often described for this type of coupling, afforded the desired dyad **3ZZ** in a moderate 36% yield. Finally Jeffery conditions,[52] using the mixture $Pd(OAc)_2$ with tetra-butyl ammonium bromide in DMF, significantly improved the yield of this reaction, since it reached 74%. The double-bond geometry in dyad **3ZZ** is *trans*, as evidenced by the large coupling constants of the vinyl moiety ($^3J = 16$ Hz). Finally, a Sonogashira cross-coupling reaction between two equivalents of bisethynyl quaterthiophene **18** and one equivalent of iodoporphyrin **10** following Lindsey conditions[53] led to the bisporphyrin **4ZZ** in 56% yield. When equimolar amounts of **18** and **10** were reacted under the same conditions, the major product was **4Z**, in which the quaterthiophene is coupled to one porphyrin unit. This synthon can be subsequently used in a second Sonogashira cross-coupling reaction in order to graft a second porphyrin module, allowing thus the stepwise construction of a asymmetrical bisporphyrin system.

Asymmetrical dimers **ZH** were prepared for studying the photoinduced energy transfer from zinc porphyrin to free-base porphyrin. To this end, demetalation of the biszinc dimer was achieved with few drops of concentrated hydrochloric acid in chloroform. Then, monometalation of the bis-free-base dyad was performed with one equivalent of zinc acetate in a chloroform/methanol mixture under reflux. The course of the reaction was monitored by TLC, and it was stopped before the concentration of the biszinc dyads became significant. The mixture of the three porphyrins **ZZ**, **ZH**, and **HH** was separated by preparative TLC to afford the pure monozinc metalated dyad **ZH**.

The structures of these new porphyrin dyads were determined with both 400 MHz ^{1}H NMR spectroscopy and high-resolution electrospray mass spectrometry. As an example, part of the ^{1}H NMR spectrum of the dyad **4ZH** is presented in Figure 1. It is interesting to note that the magnetic nonequivalence of the protons born by the zinc porphyrin is sufficiently large, relative to those of the free-base porphyrin, to give distinct signals; thus each porphyrin unit displays its own signature in the spectrum. The protons of the zinc porphyrin are noticeably more deshielded than those of the free base, probably due to a stronger ring current in the former.

For the zinc porphyrin, protons H_{3Zn} and H_{2Zn} appear at $\delta =$ 9.78 and 9.05 ppm, respectively, as two doublets ($^3J = 4.8$ Hz) due to their mutual coupling; whereas in the free-base porphyrin unit these doublets appear, respectively, at $\delta =$ 9.68 and 8.94 ppm. β-Pyrrolic protons H_{12} and H_{13} are in a very similar magnetic environment, and give rise to an AB quartet at $\delta = 9.91$ and 8.80 ppm for the zinc and the free-base porphyrin, respectively. The different chemical environment of the *meso*-phenyl groups in position 15 compared with those in positions 10 and 20 brings about different chemical shifts for the *ortho*, *para*, and *tert*-butyl hydrogens of these substituents. As expected, the surface ratios of these sets of resonances are found to be consistently equal to ½. The *ortho* hydrogens give a doublet ($\delta = 8.04$, $^4J = 1.8$ Hz) and the *para* hydrogens give a triplet ($\delta = 7.8$, $^4J = 1.8$ Hz). Here again the magnetic independence of the protons of the zinc porphyrin relative to the free-base unit can be clearly observed for the *ortho* protons, since they appear as four distinct doublets ($\delta =$ 8–8.1 ppm). The quaterthiophene protons H_4 and $H_{4'''}$ closest to the porphyrin rings give two different singlets that are relatively deshielded relative to the other protons of the spacer ($\delta = 7.55$ and $\delta = 7.56$). This is certainly a consequence of the magnetic field created by the porphyrin ring current, which is only significant at short distance. The other quaterthiophene protons ($H_{3'}$, $H_{4'}$, $H_{3''}$, $H_{4''}$) give doublets around the residual nondeuterated chloroform solvent. The rest of the spectrum is rather simple, it exhibits a triplet at $\delta =$ 2.94 ppm, assigned to the methine groups attached to the quaterthiophene in positions 3 and 3‴. At $\delta = 1.5$ ppm, *tert*-butyl groups appear as two intense singlets. The rest of the alkyl-side-chain protons born by the spacer give large multiplets in this region. As usual, the inner NH protons appear as a strongly shielded singlet at $\delta = -2.17$ ppm, whose integral corresponds to two protons in agreement with a monometalated dyad.

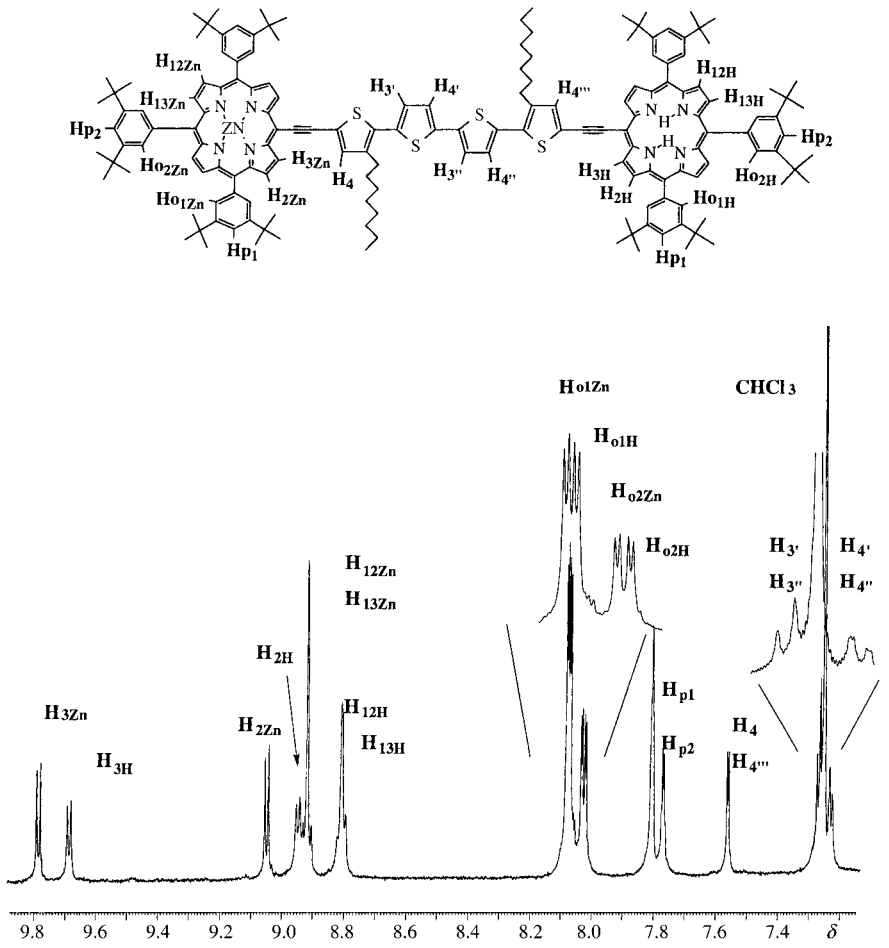

Figure 1. Aromatic region of the ^{1}H NMR spectrum of the dyad **4ZH** recorded in $CDCl_3$.

Electronic absorption spectroscopy: The electronic communication between the porphyrins in the dyads according to the nature of the linkers is of particular relevance to the present work. UV-visible absorption can be used to determine the magnitude of the interporphyrin interactions.

Figure 2 shows the electronic absorption spectra of **1ZZ**–**4ZZ** in dichloromethane together with that of the reference zinc porphyrin **7**. There are significant differences between the absorption spectra of dyads **1**–**4**; this reflects the alteration of the degree of interporphyrin electronic interaction through the linker.

Very few differences between the absorption spectra of **1ZZ** and **2ZZ** and the spectrum of the reference zinc porphyrin **7** are observed. The absorption maxima are not modified, and the spectra of the two dyads are simply the sum of the respective chromophores: the porphyrin and the oligothiophene bridge. The latter gives a transition located in the region of the Soret band of the porphyrin, which results in a broadening of the absorption band of this dyad as compared with the reference porphyrin **7**. These results indicate that direct attachment of the oligothiophene unit to the porphyrin gives practically no perturbation of the ground state properties of the porphyrin moiety.

The absorption spectra of dyads **3ZZ** and **4ZZ** display a number of interesting characteristics that are in sharp contrast to the dyads **1ZZ** and **2ZZ**. Inserting a vinyl or an ethynyl group between the quaterthiophene linker and the porphyrin core imparts distinctive features to the optical spectrum of the dyad relative to the reference. The Soret band in **3ZZ** and **4ZZ** is noticeably broadened compared with **1ZZ** and **2ZZ**. A red shift of the Q-bands along with a considerable increase in their intensity relative to the Soret band can also be observed. In dyad **4ZZ**, the Soret band even displays more than one discernible transition and is red-shifted.

The dyad **4ZZ** undergoes the largest red shift and the highest intensification of the Q-bands within the series. In this region, the spectra closely resemble those for other structurally very similar ethynyl-substituted Zn^{II} porphyrins.[20, 21, 54] The observed differences compared with the dyads **1ZZ** and **2ZZ** can therefore be attributed mainly to the effect of the ethynyl substituent, without any substantial influence of the quaterthiophene bridge. Furthermore, the spectrum in the Q-band region for **4ZH** is just the sum of the spectra for **4ZZ** and **4HH**. Similarly, the spectrum in the Q-band region for **4ZZ** and the reference compound **4Z** are identical in shape. Thus, there is no effect of

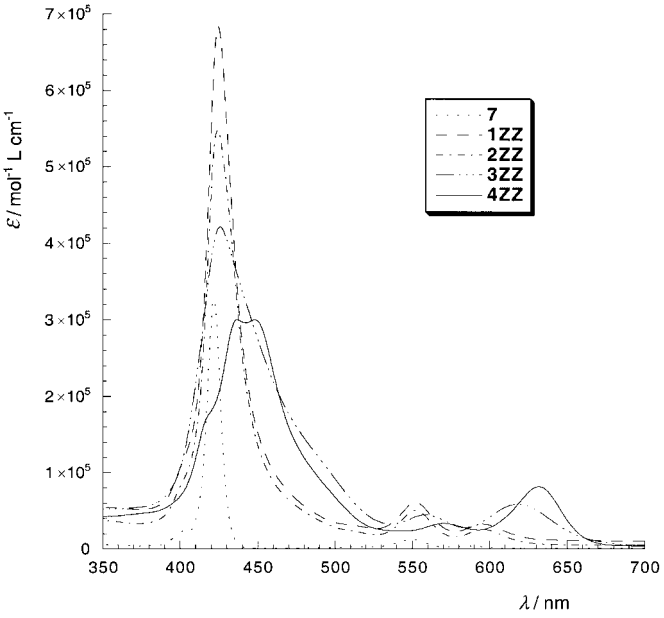

Figure 2. Electronic absorption spectra of dyads **1ZZ**–**4ZZ** and zinc monomeric porphyrin **7** recorded in dichloromethane.

  0947-6539/02/0813-3032 $ 20.00+.50/0 *Chem. Eur. J.* **2002**, *8*, No. 13

interactions between the porphyrin units in this spectral region. The bathochromic shifts can be explained as a decrease in the gap between the highest occupied molecular orbital (HOMO) and the lowest unoccupied molecular orbital (LUMO) as a consequence of the enlargement of the π-conjugated system. This is also observed in the shift of the fluorescence band toward the lowest energy level (vide infra). The results for the dyads **3ZZ**, **3HH**, and **3ZH** can be summarized and interpreted similarly, although the Q-band red-shift due to the vinyl substituent is somewhat smaller than that for ethynyl.

The Soret region of the spectrum for dyads **4** displays more variations, as shown in Figure 3 for **4HH**, **4ZZ**, and **4ZH**, together with the monozinc porphyrin linked to acetylenic quaterthiophene **4Z**. For **4ZZ** two peaks at 437 and 448 nm

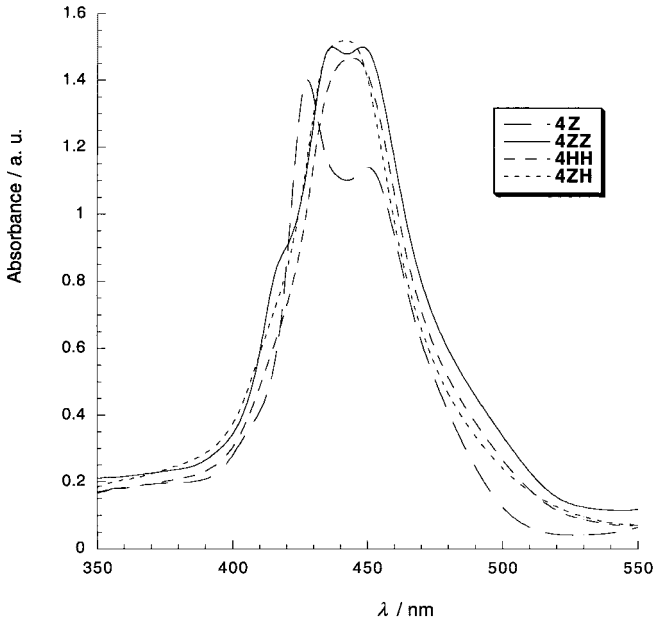

Figure 3. Soret band region of the electronic absorption spectra of compounds **4Z**, **4ZZ**, **4ZH**, and **4HH** in CH_2Cl_2.

and a shoulder at 417 nm can be seen. In contrast, **4HH** and **4ZH** display single maxima, at 442 and 444 nm, respectively. The Soret region for **4Z** shows an asymmetric feature with a narrow peak at 428 nm and a smaller, somewhat broader peak at 450 nm. If the complicated Soret region structure for **4ZZ** were only due to electronic interaction with the quaterthiophene bridge, then **4ZZ** and **4Z** would have nearly identical spectra, but this is not the case. Also, the **4ZH** spectrum would be just the sum of the spectra for **4ZZ** and **4HH**, which is not true in the Soret region. We also note that the full width at half maximum height (fwhm) of the Soret bands is about 20% larger for **4ZZ** than for **4HH**, **4ZH**, and **4Z**; this is a sign of ZnP–ZnP electronic interaction in **4ZZ**. Thus, we conclude that the electronic interaction between the ZnP units of **4ZZ** is strong enough to give detectable spectral changes in the Soret region. This demonstrates the strong electronic communication promoted by the bridge in this dyad, as also indicated by the calculations and the fluorescence results (vide infra). From comparison with related bisporphyrin dyads,[20, 21, 54] it seems that a direct excitonic interaction between the porphyrins at this distance would be too weak to explain the spectral changes in **4ZZ**. Other electronic interactions that arise from direct orbital overlap mediated by the bridge may instead explain the spectrum. These results show that there is an increasing degree of electron delocalization within the series that becomes particularly significant for dyads **3ZZ** and **4ZZ**.

In **4Z**, the narrow band at 427 nm can be attributed to a ZnP transition that is slightly red-shifted due to the ethynyl group. The 450 nm band can probably be assigned to the quaterthiophene absorption, that is red-shifted from the normal 404 nm due to the same ethynyl group. Any significant excitonic interaction between the porphyrin and the quaterthiophene is unlikely due to the low extinction coefficient of the latter ($28000\,M^{-1}cm^{-1}$). The bridge-localized transition at 448 nm in **4HH** and **4ZH** cannot be distinguished because it is covered by the Soret band of the free-base porphyrin unit in these two dyads.

Spectra of bis-free-base dyads exhibit the same types of characteristics as those met with biszinc dyads, therefore similar conclusions can be drawn for these systems (Figure 4). It is however interesting to note that in the bis-free-base dyads **3HH** and **4HH**, the attachment of double or triple bonds

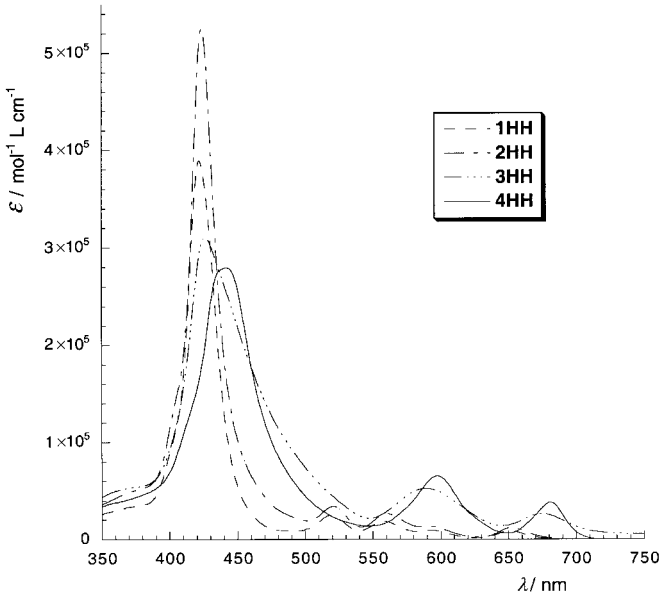

Figure 4. Electronic absorption spectra of dyads **1HH**–**4HH** in CH_2Cl_2.

greatly increases the oscillator strength of the Q(0,0)-bands, and also seems to reduce somewhat the intensity of the Q(1,0)-bands. The modification of the relative intensity of the Q(0,0) and Q(1,0) absorption transitions is also observed in the biszinc dyads (Figure 4), although for these dyads the result is only an increase in the Q(0,0) intensity, while the Q(1,0) transition strength appears unaffected and can still be clearly resolved. Changes in the relative transition strengths for Q(0,0)- and Q(1,0)-bands have been explained by Gouterman:[56] Abs[Q(0,0)]/Abs[Q(1,0)] is proportional to the square of the energy difference $E(a_{2u} - e_g) - E(a_{1u} - e_g)$, in which the latter corresponds to the energies of the singlet transitions. Thus, the small Q(1,0)-bands indicate that the

energy difference between singlet transitions is relatively large in dyads **3** and **4** compared with the case in dyads **1** and **2** or in 1,5,10,15-tetrakis(phenyl)porphyrin (TPP). This most probably results from the attachment of a bridge at the 5 *meso* position, which electronically communicates with the porphyrin core. The asymmetry induced by the vinyl or ethynyl groups lifts the degeneracy of the LUMO (e_g). Furthermore, at this position the a_{1u} orbital has a node, but the a_{2u} orbital may be stabilized by the conjugated substituent. This will affect the energy of these orbitals differently. These effects may explain the observed change in the relative intensity of the Q(0,0)- and Q(1,0)-bands. The increase in the Q(0,0)-band(s) occurs at the expense of the Soret band intensity (Figure 2), as expected, while the relatively constant intensity of the Q(1,0)-band(s) is in agreement with their deriving oscillator strength mainly through intensity borrowing from the higher (Soret) transition.[56]

The spectra of the asymmetrical dyads **1ZH**–**3ZH** are clearly superpositions of the spectra of the corresponding biszinc and bis-free-base dyads. As illustrated for dyad **2ZH** in Figure 5, the spectrum can be approximated by a linear combination of the absorption spectra of **2ZZ** and **2HH**. This indicates that the attachment of a free-base or of a zinc porphyrin at the spacer termini has little influence on the ground-state electronic structure of the dyads. The case is different for **4ZH**, for which the Soret region is not given by the sum of the spectra for **4HH** and **4ZZ** (vide supra).

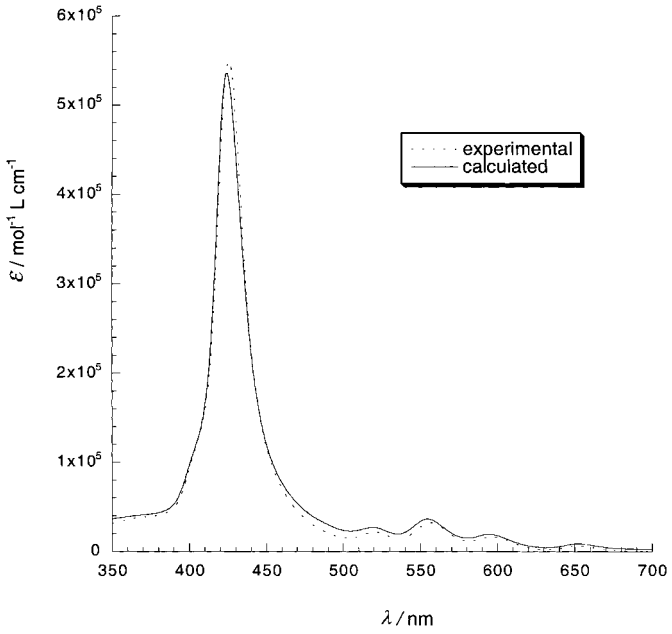

Figure 5. Electronic absorption spectrum of dyad **2ZH** in CH_2Cl_2. Experimental spectrum (----), calculated (----) as the half sum of the spectra of **2HH** and **2ZZ**.

The bisporphyrin systems **1** and **2** show very small spectral differences compared with the model porphyrins, while the dyads **3** and **4** exhibit absorption spectra that are significantly altered relative to the monomeric porphyrin. As a result, the latter dyads are true supermolecules, because their electronic properties differ from the isolated pigments as a consequence of interchromophoric electronic coupling between the porphyrin and the quaterthiophene bridge and, for **4ZZ**, also between the two porphyrin units.

These results demonstrate that the nature of the bridge and particularly the type of connectivity between the porphyrin and the thiophene has a deep impact on the magnitude of the interchromophore interactions. From the absorption spectra, it can be concluded that the quaterthiophene bisacetylenic bridging unit in dyad **4** provides the most efficient electron delocalization and therefore the largest electronic interaction between the two porphyrins. Further support for this conclusion comes from the computational and fluorescence studies discussed below.

Computational studies: Molecular orbital calculations were undertaken to rationalize the observed UV-visible absorption behavior in this series of porphyrin dyads, and to gain a better understanding of how the linkage modulates the electronic interactions. Calculations were performed by using semi-empirical AM1 theoretical model as incorporated in the SPARTAN program. This type of calculation has already been conducted for other porphyrin arrays and proved to be reliable for the determination of geometrical parameters.[16, 57] In order not to exceed the maximum number of atoms for this type of program, calculations were performed on less substituted analogues: the octyl chains on quaterthiophene and the *tert*-butyl substituents on *meso*-phenyl were replaced by a methyl and a hydrogen, respectively. To limit the number of figures, the discussion of this part will be conducted on biszinc dyads **1ZZ**–**4ZZ**, since very similar conclusions can be drawn from the other sets of bisporphyrins. The optimized geometries of the dyads **1ZZ**–**4ZZ** are presented in Figure 6.

The conformations of the molecules are very different in the four dyads. In these structures, the dihedral angle (α) between the porphyrin core and the first thiophene appended to the bridge is close to 90° for dyads **1** and **2**, 52° for dyad **3**, and 0° for dyad **4** (Table 1). The dihedral angle (β) between the central thiophenes has a value of 20° for dyad **1** and decreases from dyads **1** to **4**. The dihedral angle (γ) between the second and the third thiophene units of a quaterthiophene is close to 0° degree in all molecules.

Table 1. Geometrical data within the dyads.

Dyads	d_1[a] [Å]	d_2[b] [Å]	α[c] [°]	β[d] [°]
1ZZ	9.1	16.0	87	20
2ZZ	16.8	23.6	85	32
3ZZ	21.6	28.4	52	30
4ZZ	21.8	28.6	0	24

[a] d_1 = edge-to-edge distance between the porphyrins. [b] d_2 = center-to-center distance between the porphyrins. [c] α = dihedral angle between the porphyrin and the first thiophene of the bridging unit. [d] β = dihedral angle between the two central thiophenes.

Steric interactions between the β-pyrrole proton of the porphyrin ring and the *ortho* proton of the thiophene in **1** and **2** force these segments to adopt a nearly orthogonal orientation with respect to the porphyrin macrocycle; this interrupts the conjugative pathway between the porphyrin macrocycle and the linker.

  0947-6539/02/0813-3034 $ 20.00+.50/0 *Chem. Eur. J.* **2002**, *8*, No. 13

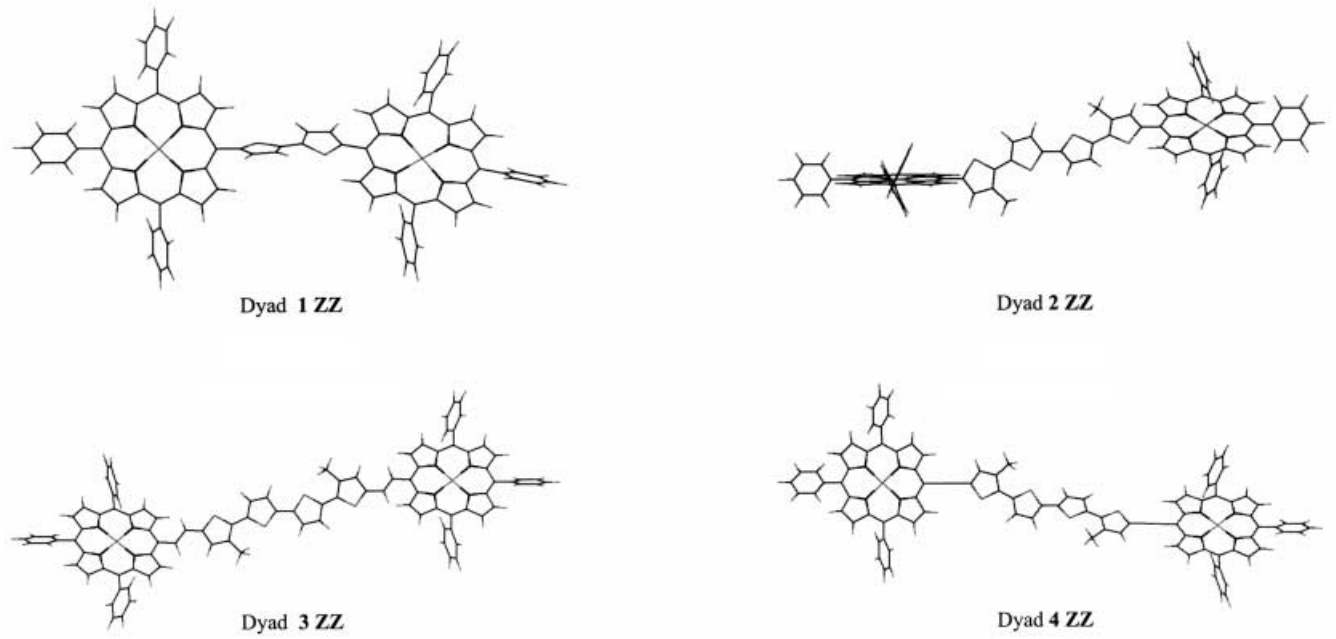

Figure 6. Optimized geometries of the dyads calculated with the AM1 semiempirical method.

In marked contrast to dyads **1** and **2**, the porphyrins and the oligothiophene bridge of dyad **4** lie in a same plane, because the distance between the β-thiophene protons and the β-pyrrole protons is sufficiently long to prevent steric hindrance. Therefore, one of the features of the triple bond is to remove the steric constraint by pushing the porphyrin and the thiophene moieties further apart. This geometry enables the frontier orbitals of the thiophene linker to overlap with those of the porphyrin macrocycle and results in an increase in the π-conjugated system.

An intermediate situation can be found in dyad **3**. In this array, the dihedral angle α is 52° owing to the existence of partial steric interactions between the ethylenic protons of the spacer and those of the pyrrolic units. This hindrance is less than that observed in dyads **1** and **2**, but is not completely removed, as in dyad **4**.

The geometrical changes observed in the structures of the dyads will have a great impact on the electron density distribution of their respective wave functions. Table 2 lists the calculated frontier-molecular-orbital energies of the dyads calculated in this study. Figures 7, 8, 9, and 10 display the representation of the frontier molecular orbitals of the four dyads **1ZZ**–**4ZZ** ordered according their respective energy.

First, the energy of the HOMO orbital is more or less constant within the whole series of dyads. This is consistent with the fact that the HOMO orbital does not bear any electron density on the *meso* carbon, where the bridge is appended, therefore the spacer has little impact on this molecular orbital. Interestingly, the LUMO and the LUMO+1 are degenerate in dyads **1** and **2** similarly to the tetraaryl reference porphyrin, as already observed in the classical Gouterman four-orbitals model.[58] This confirms that the attachment of the oligothiophene bridge induces only a small perturbation of the porphyrin electronic structure, because the energy and the electron distribution of the frontier orbitals have not changed significantly compared with the reference monomeric porphyrin. In these structures, the frontier molecular orbitals of the porphyrin core and the quaterthiophene bridge do not mix effectively. Each orbital is fully localized on each module with no distribution on the neighboring fragment. As a result, the porphyrins behave independently to one another, and can be considered as electronically distinct.

Table 2. Frontier orbital energies [eV] of the dyads **1ZZ-4ZZ**.

Molecules	**1ZZ**	**2ZZ**	**3ZZ**	**4ZZ**	**ZnTPP**	Quaterthiophene[a]
LUMO + 1	− 1.72	− 1.72	− 1.73	− 1.84	− 1.65	− 0.39 (− 0.71)
LUMO	− 1.72	− 1.72	− 1.74	− 1.85	− 1.67	− 1.03 (− 1.23)
HOMO	− 7.39	− 7.39	− 7.39	− 7.39	− 7.36	− 7.96 (− 8.00)
HOMO − 1	− 7.39	− 7.39	− 7.39	− 7.39	− 7.51	− 8.87 (− 8.75)

[a] Energy of 5,5‴-bis(ethynyl quaterthiophene **18**‴.

The calculated energy gap between the HOMOs and LUMOs within the series of dyads decreased in agreement with the bathochromic shift of the absorption and emission bands. It is generally accepted that the magnitude of electronic communication depends on the degree of overlap between the orbitals of the bridging unit and the modules.[1, 3] The other key requirement for large linker-mediated electronic communication is the energy proximity of the orbitals of the linker and those of the porphyrin; this is best matched for the LUMO orbitals in dyad **4**.

Another salient feature of dyad **4** is the bridge-localized electron density that appears in the HOMO − 1, HOMO, LUMO, and LUMO+1 orbitals. This is consistent with the planarity of the molecule, which favors the weight of this cumulenic form that requires a planar arrangement of the whole backbone. Similarly, Therien[21] and Anderson[32] have already reported that the high electronic coupling with

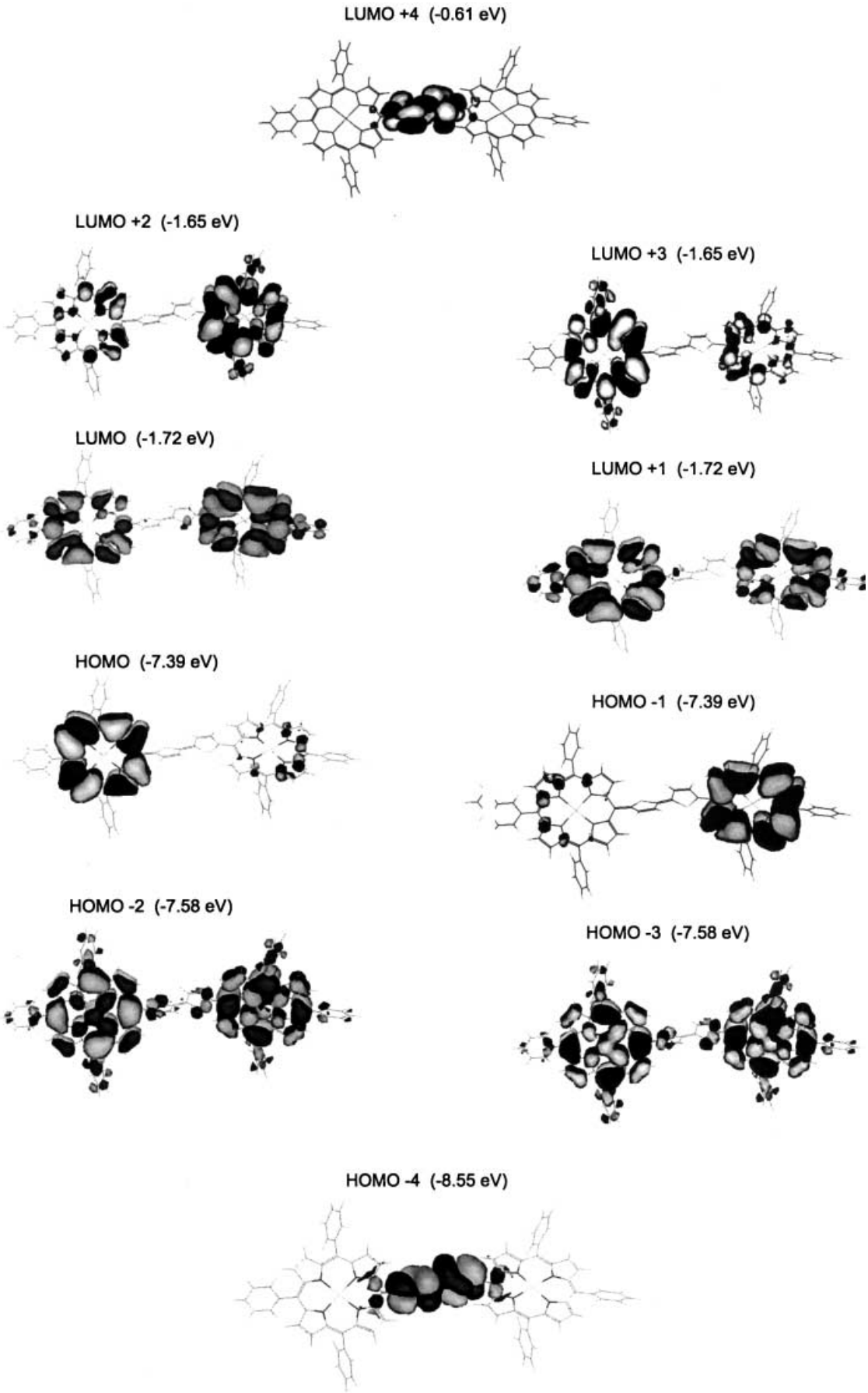

Figure 7. Frontier molecular orbital distributions in dyads **1ZZ**.

  0947-6539/02/0813-3036 $ 20.00+.50/0 *Chem. Eur. J.* **2002**, *8*, No. 13

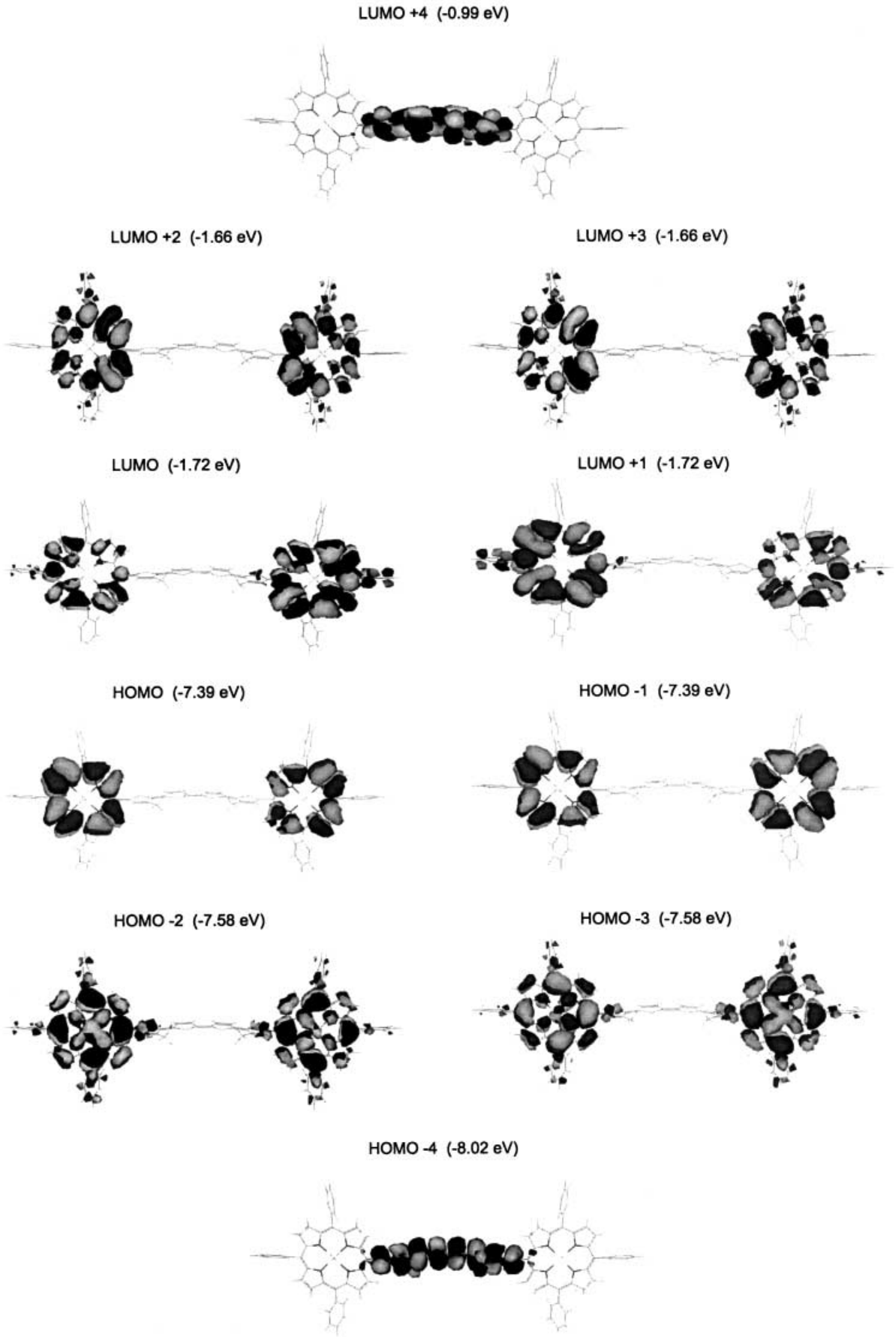

Figure 8. Frontier molecular orbital distributions in dyads **2ZZ**.

  0947-6539/02/0813-3037 $ 20.00+.50/0

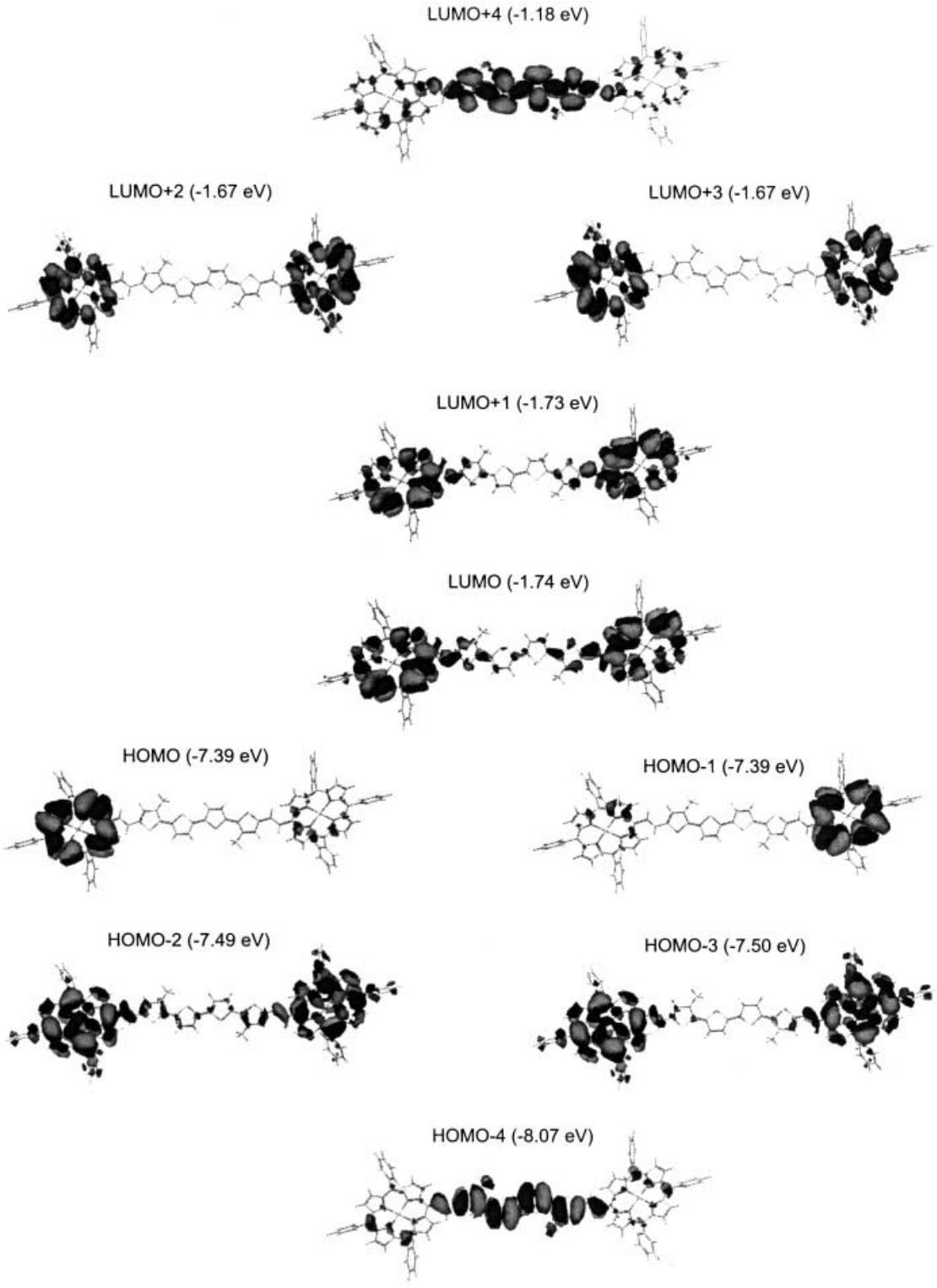

Figure 9. Frontier molecular orbital distributions in dyads **3ZZ**.

oligoethynyl chains lies in the potential cumulenic resonance structure as illustrated in Scheme 5.

As pictorially shown on the HOMO, HOMO – 1, and LUMO of dyad **4ZZ**, the electron density is distributed significantly along the axis defined by the bridge direction. This effect was also observed by Therien et al.[21] in *meso*-ethynyl-substituted porphyrins. Accordingly, the excited state of dyad **4** is most probably strongly polarized in this direction; this is favorable to photoinduced electron or energy transfer toward the adjacent porphyrin. The lowest HOMO – LUMO gap is observed for dyad **4**, in agreement with the most planar structure and our UV-visible measurements. Furthermore, the electron density distribution of the HOMO orbital shows an extensive electronic delocalization

  0947-6539/02/0813-3038 $ 20.00+.50/0 *Chem. Eur. J.* **2002**, *8*, No. 13

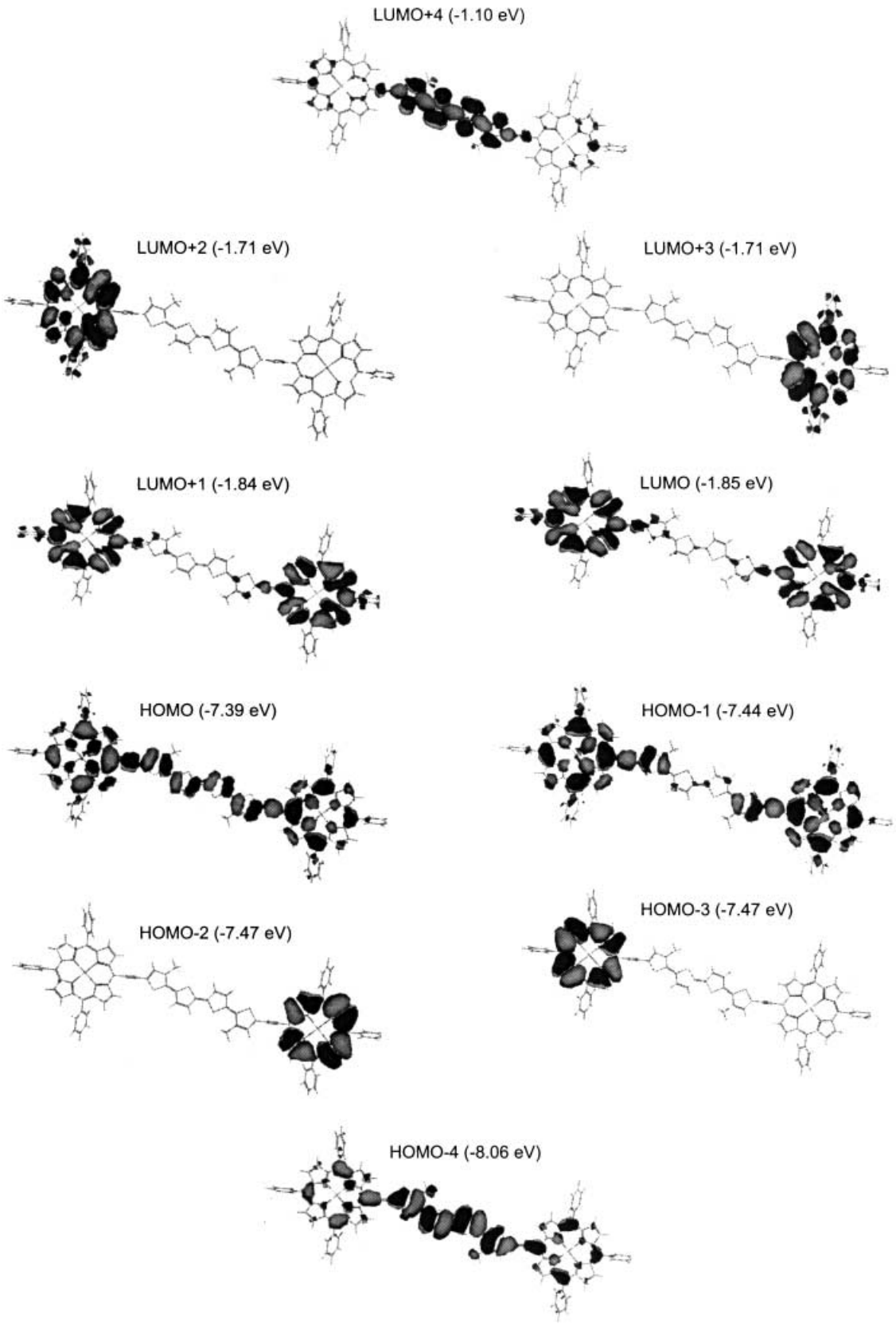

Figure 10. Frontier molecular orbital distributions in dyads **4ZZ**.

through the whole structure of dyad **4**. On the other hand, the HOMO orbital of dyad **1** or **2** is fully localized on the porphyrins moieties.

The present results lead to the conclusion that the large electronic interaction observed in dyad **4** can be explained by the nature of the quaterthiophene acetylene bridge, which

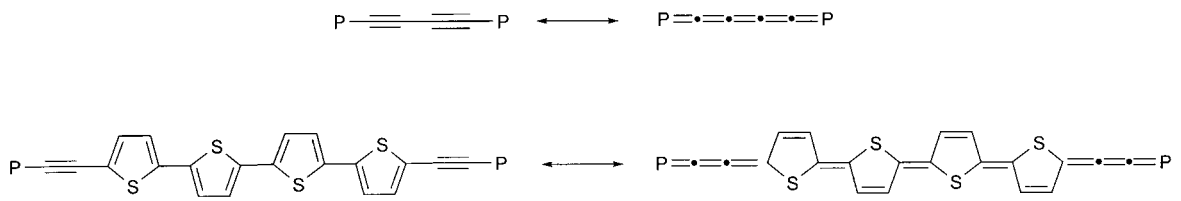

Scheme 5. Representations of the cumulene structures.

allows the porphyrin macrocycles to adopt a coplanar arrangement by removal of the steric hindrance, and probably by a correct energy matching of its molecular orbitals with those of the porphyrins.[58] The extended delocalization of the π system thanks to high mixing of each unit frontier orbital creates a conjugated pathway from one end of the molecule to the other, in which the bridge behaves as a molecular wire.

The importance of the linking element on the electronic conjugation is highlighted by the difference between dyads **1** and **4**. The interporphyrin distance is greater by a factor of more than two in dyad **4** compared with dyad **1**; however, only the former shows an efficient electronic delocalization. This demonstrates that the interchromophore electronic interaction can be promoted over a large distance by the appropriate choice of the spacer. To this end, bisethynyl quaterthiophene is particularly well suited to provide large interporphyrin interaction.

Fluorescence spectroscopy: The fluorescence maxima of all dyads are given in Table 3. The fluorescence spectra of **2ZZ**, **2HH**, **2ZH**, **4ZZ**, **4HH**, and **4ZH** are shown in Figures 11 and 12.

Table 3. Fluorescence data.

Compound	λ_{max} [nm]	τ_{fl} [ns]	Φ_{fl}	k_{ET} [$\times 10^{-10}$ s^{-1}][a]
1ZZ	624	1.6	0.10	
1HH	662	3.9	0.86	
1ZH	664	0.017[b]	0.86	6
2ZZ	626	1.3	0.085	
2HH	667	3.5	0.78	
2ZH	666	0.032[b]	0.78	3
3ZZ	676	1.3	0.17	
3HH	717	3.4	0.22	
3ZH	713	0.033[b]	0.21	3
4ZZ	657	1.4	0.18	
4HH	690	6.2	0.34	
4ZH	688	0.008[b,c]	0.31	12[c]

[a] Calculated from $k_{ET}=1/\tau_{ZH}-1/\tau_{ZZ}$, in which τ_{ZH} and τ_{ZZ} are the lifetimes of the fluorescence from the ZnP unit in the **ZH** and the **ZZ** dyad, respectively. Since $\tau_{ZH} \ll \tau_{ZZ}$, practically $k_{ET}=1/\tau_{ZH}$. [b] Fluorescence lifetime observed in the spectral region where ZnP fluorescence dominates (see Figures 11 and 12). At longer wavelengths, a much slower component dominated, with a lifetime matching that of the corresponding **HH** dyad. [c] Estimated accuracy ±40% (otherwise ±10%), due to limited time resolution.

Similarly to the absorption spectra, the nature of the bond linking the porphyrin units to the bis- or quaterthiophene bridge alters the emission characteristics of the system. This is manifested in a red shift of the fluorescence maximum as the π-delocalization of the porphyrin orbitals into the spacer increases. Note, however, that **3HH**, **3ZZ**, and **3ZH** display a

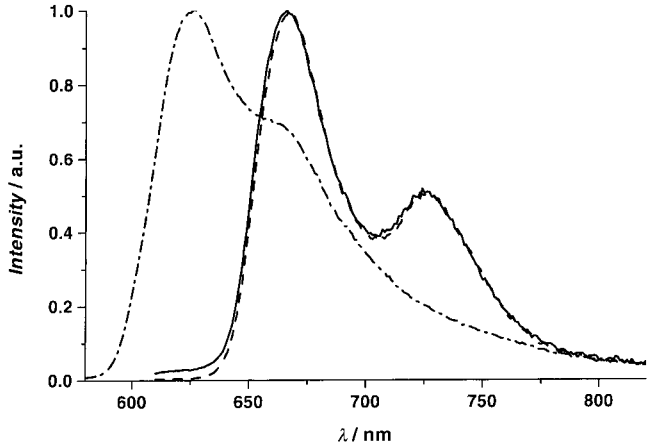

Figure 11. Corrected and normalized fluorescence spectra of dilute THF solutions of **2ZZ** (•–•), **2HH** (----) and **2ZH** (——). Excitation wavelength = 560 nm.

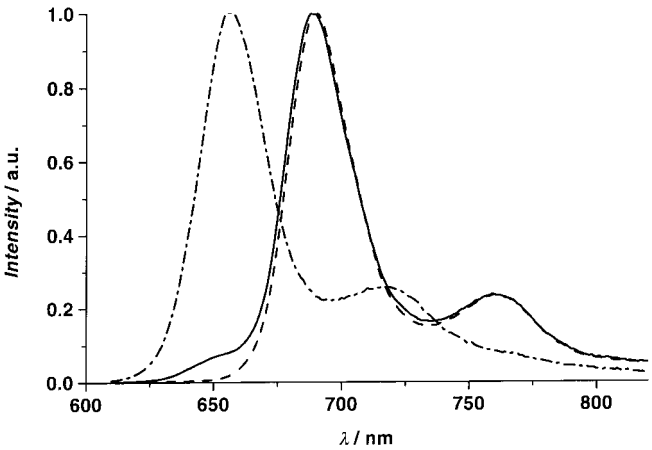

Figure 12. Corrected and normalized fluorescence spectra of dilute THF solutions **4ZZ** (•–•), **4HH** (----) and **4ZH** (——). Excitation wavelength = 560 nm.

larger Stokes shift between the lowest absorption band and the fluorescence maximum than the other dyads. This indicates that dyad **3** undergoes a significant reorganization of nuclear coordinates in the excited state. The fluorescence energy order is **1ZZ** ≈ **2ZZ** > **4ZZ** > **3ZZ**. The H2P–H2P dyads follow the same order. The fluorescence quantum yield (Table 3) for the ZnP–ZnP dyads increases in the order **2ZZ** < **1ZZ** < **3ZZ** ≈ **4ZZ**. The quantum yields for the series of H2P–H2P dyads follow a similar trend The observed fluorescence lifetimes are very similar for all the ZnP–ZnP dyads, at about 1.5 ns. This value is typical for zinc(II) tetraphenyl- or octaalkylporphyrins.[27] Since the deactivation of the fluorescent S_1 state in this type of porphyrins is

  0947-6539/02/0813-3040 $ 20.00+.50/0 *Chem. Eur. J.* **2002**, *8*, No. 13

dominated by nonradiative transitions (intersystem crossing to the T_1 state),[27] the increase in fluorescence yield must be explained by an increase in the radiative rate constant, k_r. This explanation is consistent with the increase in transition probability (extinction coefficients) observed for the lowest energy Q-band (Figures 2 and 4).

Photoinduced energy transfer was investigated in the asymmetrical zinc(II)/free-base porphyrin dyads **ZH**. The energy of the lowest singlet excited state (S_1) in the zinc(II) porphyrins is higher than for the corresponding free-base porphyrin. Excitation of the ZnP–H_2P dyads at 560 nm, at which most of the light is absorbed by the zinc porphyrin unit, gave fluorescence spectra in which >98% of the emission (>95% for **4ZH**) is from the free-base porphyrin unit (Figures 11 and 12).

The excitation spectra of optically dilute samples (Abs < 0.1) are in very good agreement with the absorption spectra, in both the Soret band and Q-band regions (not shown). In addition, the fluorescence quantum yield is identical for a **ZH** dyad and the corresponding **HH** dyad (Table 3), within experimental error. Thus, the yield of free-base porphyrin fluorescence is as high when the zinc porphyrin is excited as when the free-base porphyrin itself is excited. These results indicate that energy transfer from the former to the latter is >98% efficient. The small residual ZnP emission in the fluorescence spectra of the asymmetrical dyads can be ascribed to a small amount of unquenched ZnP impurity.[59]

The lifetime of the zinc porphyrin fluorescence in the symmetrical and asymmetrical dyads is given in Table 3. The lifetime is strongly reduced in the asymmetrical dyad, from about 1.5 ns in the symmetrical dyad to around 30 ps or less. This is consistent with the efficient energy transfer to the free-base porphyrin moiety deduced from the fluorescence spectra above. The energy transfer rate constants were calculated as $k_{EnT} = 1/\tau - 1/\tau_0$; here τ and τ_0 are the zinc porphyrin fluorescence lifetimes in the asymmetrical and the symmetrical dyads, respectively. The order of the energy transfer rate constants is **2ZH** ≈ **3ZH** < **1ZH** < **4ZH**. The calculated rate constants for a coulombic (Förster) mechanism[60] are lower than those observed, and do not predict the relative rate. In particular, the observed rate constant for **4ZH** is more than an order of magnitude larger than the calculated one. Thus, energy transfer presumably occurs mainly by a bridge-mediated exchange energy transfer, and for **4ZH** this definitely seems to be the case. With this mechanism, the rate decreases exponentially with distance. The rate order observed is consistent with the opposing effects of more delocalized excited states for **3ZH** and **4ZH**, but also longer porphyrin–porphyrin distances than in **2ZH** and **1ZH**. The fact that the dyad with the longest interchromophoric distance (28.6 Å center-to-center in **4ZH**) has the fastest energy transfer shows again the good electronic communication mediated by this bridge.

Conclusion

The synthesis of dyads composed of porphyrins connected with four types of oligothiophene bridges has been presented. The preparation of these compounds was achieved according to a modular approach by using *meso*-iodotriarylporphyrin **9**. The ability to substitute this porphyrin with various connectors by using the three types of cross-coupling reactions: Stille, Heck, and Sonogashira demonstrates the high versatility of this synthetic approach, which provides access to large porphyrin arrays with a wide variety of different bridges.

In order to identify the most useful connector in terms of interporphyrin electronic coupling, we investigated the dyads **1**–**4** by UV-visible absorption spectrometry and by fluorimetry. These data have been rationalized by AM1 semiempirical calculations.

The absorption spectra of **1** and **2** are essentially invariant with respect to the zinc porphyrin reference. This indicates that the porphyrins in these dyads are essentially electronically decoupled in the ground state. We infer that the end thiophene units of the wire that links the dyad lie approximately orthogonal to the chromophores, and prevent overlapping of the porphyrins orbitals with those of the bridge. Red shifts of the absorption bands observed in dyads **3** and **4** were ascribed to a large electronic coupling between the two chromophores and the bridge. In comparison with **4**, the optical spectrum of **3** does not exhibit as great a broadening of the Soret band neither as strong a red shift of the Q-bands; this indicates that dyad **3** displays an intermediate behavior between **1/2** and **4**. As a consequence, it is interesting to note that the introduction of a vinyl group between the porphyrin and the quaterthiophene bridging unit is not as significant as the introduction of an ethynyl group. This means that the oligomerization of four thiophene units with an acetylene moiety at the *meso* position of the porphyrin core forms the best bridge to provide propagation of the electronic interactions within two zinc porphyrins. In dyad **4**, the coplanarity of the whole system ensures a large degree of overlap of the orbitals of each fragment, hence a delocalization of the π system over the whole molecule. From fluorescence emission spectroscopy, the energy difference between the HOMO and LUMO can be ranked in the order: **1HH** ≈ **2HH** > **4HH** > **3HH**. It is important to note that these arrays display significant electronic communication without large perturbations of the electronic properties of the porphyrin constituents. Indeed the lifetimes and energy levels of the excited states are not reduced to a large extent and, more importantly, the excited state of each porphyrin module remains an individual separate state.

Varying the linker structure in these series of dyads enabled us to tune the interporphyrin interactions, thereby providing the means to investigate the dependence of the photoinduced energy-transfer rate on the chemical structure of the linker. Thus, the energy transfer in asymmetrical **ZH** dyads was studied by fluorescence spectroscopy. The fluorescence of the zinc porphyrin is almost entirely extinguished in each **ZH** dyad, and instead the free-base porphyrin fluorescence is sensitized. This indicates that the zinc porphyrin excited state is efficiently quenched by the nearby free-base porphyrin due to a fast and efficient energy transfer. The ZnP fluorescence lifetime decrease indicates a clear trend from the slowest to the fastest energy transfer rate: **2ZH** ≈ **3ZH** < **1ZH** < **4ZH**. The fast and efficient photoinduced energy-transfer process in

the dyad **4ZH** probably includes the participation of the thiophene bridge and may proceed by a predominantly Dexter type mechanism; this implies a double-electron self-exchange, since the calculated Förster rate constant[60] is an order of magnitude lower than the observed one. Although the separation distance between the two porphyrin modules is largest in dyad **4**, the photoinduced energy process of this dyad had the highest rate within the series. For such a long separation, the high rate constant observed in dyad **4ZH** is among the fastest values reported so far in linked bisporphyrin systems.[28, 55, 61]

This work demonstrates new compelling evidence that strong electronic communication can be promoted over large distance and is beneficial to achieving long-range and efficient photoinduced processes. It confirms the merit of the approach that consists of developing coupled chromophoric arrays for long-range energy migration or charge separation. Thus, although the orbitals of the two distant porphyrins cannot overlap appreciably with each other because of the large separation distance, they can overlap to a great extent with the orbitals of the bridge. This orbital overlap produces an indirect but effective mixing of the two porphyrins that yields a large interporphyrin electronic coupling even over large separation distances.

This study highlights the crucial importance of the structure of the bridge used to connect modules on the electronic interactions. The electronic coupling attenuation with distance can vary greatly within the same family of bridges if the planarity of the structure is not conserved. The present investigations show that oligothiophene attached via an acetylene group is a viable bridging module to promote high electronic coupling between porphyrin units that can be suitable for the construction of artificial photosynthetic systems and related devices. Further work involving this latter bridge with different electron donor/acceptor porphyrin combinations is underway in our laboratory.

Experimental Section

General methods: ^{1}H NMR spectra were recorded on an ASPEC Bruker 200 MHz or a ARX 400 MHz Brucker spectrometer. Chemical shifts for ^{1}H NMR spectra are referenced relative to residual protium in the deuterated solvent ($CDCl_3$, $\delta = 7.26$ ppm). UV-visible absorption spectra were recorded on a Cary 5G Varian spectrophotometer. Low-resolution mass spectra were recorded on an EI-MS H_P5989A spectrometer. High-resolution mass spectra were recorded on a JMS-700 (JEOL Ltd, Akishima, Tokyo, Japan) double-focusing mass spectrometer of reversed geometry equipped with electrospray ionization (ESI) source. Thin-layer chromatography (TLC) was performed on aluminum sheets precoated with Merck 5735 Kieselgel 60F_{254}. Column chromatography was carried out either with Merck 5735 Kieselgel 60F (0.040 – 0.063 mm mesh) or with SDS neutral alumina (0.05 – 0.2 mm mesh). Preparative thin-layer chromatography was carried out on glass plates coated with silica gel 60G (Merck). Air-sensitive reactions were carried out under argon in dry solvents and glassware. Chemicals were purchased from Aldrich and used as received. 2-bromo-3-octylthiophene,[62] 5,5′-bis(tributyltin)-2,2′-bithiophene,[63] 3,5-di*tert*-butylbenzaldehyde,[64] 3,5-di*tert*-butylphenylboronic acid,[46] 5-iodo-10,15,20-tris-(3,5-di*tert*-butylphenyl)zinc porphyrin (**10**)[43] and tris(dibenzylideneacetone)dipalladium chloroform[65] were prepared according to literature methods.

Computational methods: The AM1 semiempirical Hamiltonian[66] was used as implemented in the quantum mechanical programs Spartan 5.1[67] and HyperChem 5.1.[68] The building blocks used to construct the various dyads studied in this work were taken from the CSD database. The refcodes of the porphyrin and quaterthiophene structures selected are, respectively, GOBSUL[69] and ZORNUP.[63] All geometries were completely optimized, that is, no restrictions in geometry were assumed, and all degrees of freedom were optimized.

Fluorescence measurements: All fluorescence measurements were performed in tetrahydrofuran (Merck, spectroscopic grade). Fluorescence spectra were recorded on a SPEX Fluorolog II Systems fluorimeter and were corrected for the wavelength-dependent response of the detector system. Fluorescence lifetimes were determined by using time-correlated single-photon counting TCSPC). The excitation light was the 560 nm output from an Optical Parametric Amplifier (Coherent), pumped by a titanium – sapphire oscillator (Mira)/regenerative amplifier system (Coherent). The pulses were typically 150 fs (fwhm) with a repetition frequency of 200 kHz and attenuated to a power of < 1 mW at the sample. The emission was selected with a suitable combination of filters and focused on a microchannel plate (MCP) detector. For the zinc(II) porphyrin emission in the asymmetric dyads, the filters employed transmitted light at 590 – 630 nm. The instrumental response function was recorded by using a scattering sample, and was typically 100 ps (fwhm). The emission-decay curves for the symmetric dyads were fitted to a single exponential function. For the zinc(II) porphyrin emission in the asymmetric dyads, the decays were fitted to a sum of two exponents, by using an iterative reconvolution with the response function. The fast component ($\tau = 10 – 30$ ps) represented the zinc(II) porphyrin fluorescence decay in the dyads, while the slow component ($\tau =$ a few ns) represented fluorescence from the free-base porphyrin unit reaching the detector. The short lifetimes of the ZnP-unit fluorescence in the asymmetrical **ZH** dyads were also measured with a streak camera (Hamamatsu Model C5680, synchroscan mode). The frequency-doubled pulses from the Mira at 400 nm (< 100 fs width, 75 MHz repetition frequency, 50 mW power at the sample) were focused on the sample. The fluorescent light at right angles was focused on the streak camera slit, passing a filter combination transmitting light at 590 – 630 nm. The response function was determined to about 4 ps (fwhm). The lifetimes determined by this method were in excellent agreement with those determined by TCSPC with the MCP detector.

3,3‴-bis(octyl)-2,2′:5′,2″:5″,2‴quaterthiophene (13): In a dry schlenk tube, $Pd_2(dba)_3 \cdot CHCl_3$ (26 mg, 25 mmol), PPh_3 (158 mg, 0.60 mmol) and a mixture of THF/DMF (1:1, 10 mL) were degassed in a ultrasound bath for 20 minutes. 5,5′-Bis(tributyltin)-2,2′-bithiophene (1.49 g, 1.74 mmol) and 2-bromo-3-octylthiophene[24] (1.08 g, 3.95 mmol) were added to this solution, which was degassed for another 20 minutes. The mixture was heated in an oil bath at 75 °C for 2 days. The crude reaction mixture was diluted with dichloromethane and washed with water. The organic layer was dried over $MgSO_4$, and the solvent was rotary evaporated. The resulting oil was purified by column chromatography over silica gel eluted with petroleum ether to yield quaterthiophene (808 mg, 84 %). ^{1}H NMR (200 MHz, $CDCl_3$, 25 °C): 0.87 (t, $^3J = 5.4$ Hz, 6H; CH_3 alkyl chain), 1.26 (m, 20H; CH_2 alkyl chain), 1.68 (m, 4H; CH_2 alkyl chain), 2.77 (t, $^3J =$ 6.8 Hz, 4H; CH_2 thioph.), 6.93 (d, $^3J = 5.2$ Hz, 2H; H_4), 7.01 (d, $^3J = 3.8$ Hz, 2H; $H_{3'}$), 7.12 (d, $^3J = 3.8$ Hz, 2H; $H_{4'}$), 7.17 (d, $^3J = 5.2$ Hz, 2H; H_5); UV/Vis. (CH_2Cl_2): λ_{max} (ε) = 404 (28 000); EI-MS m/z (%): 554 (100) [M^+], 455 (40), 323 (23); elemental analysis calcd (%) for $C_{32}H_{42}S_4$: C 69.26, H 7.63, S 23.11; found: C 69.24, H 7.75, S 23.01.

5,5‴-dibromo-3,3‴-bis(octyl)-2,2′:5′,2″:5″,2‴quaterthiophene (14): In a three-necked round-bottomed flask, a solution of quaterthiophene **13** (180 mg, 0.32 mmol) in CS_2 (20 mL) was degassed under argon. The mixture was cooled to -20 °C and a NBS solution (104 mg, 0.58 mmol) in $CHCl_3$ (50 mL) was added dropwise under argon over 1 h. The mixture was stirred at this temperature for half an hour more, then brought to 0 °C and stirred for another 30 minutes. The CS_2 was removed by a stream of air. The reaction mixture was added to a cold ammonium chloride solution, extracted with dichloromethane, and washed with water, and the organic phase was dried over $MgSO_4$.The solvent was removed by rotary evaporation, and the resulting green solid was purified over silica with petroleum ether to yield **14** (218 mg, 96 %). ^{1}H NMR (200 MHz, $CDCl_3$, 25 °C): 0.87 (t, $^3J = 5.4$ Hz, 6H; CH_3 alkyl chain), 1.26 (m, 20H; CH_2 alkyl chain), 1.68 (m, 4H; CH_2 alkyl chain), 2.70 (t, $^3J = 6.8$ Hz, 4H; CH_2 thioph.), 6.90 (s, 2H; H_4), 6.96 (d, $^3J = 3.8$ Hz, 2H; $H_{4'}$), 7.10 (d, $^3J =$

  0947-6539/02/0813-3042 $ 20.00+.50/0 *Chem. Eur. J.* **2002**, *8*, No. 13

3.8 Hz, 2H; $H_{3'}$); EI-MS *m*/*z* (%): 712 (100) [M^+], 612 (55), 513 (25); elemental analysis calcd (%) for $C_{32}H_{40}Br_2S_4$: C 53.93, H 5.66, S 18.00; found: C 54.32, H 6.01, S17.72.

5,5‴-bis(trimethylstannyl)-3,3‴-bis(octyl)-2,2′:5′,2″:5″,2‴quaterthiophene (15): Quaterthiophene **13** (190 mg, 0.34 mmol) was dissolved in anhydrous THF (10 mL) and *n*BuLi (0.34 mL, 2.5 M solution in pentane) was added dropwise at −78 °C. The mixture was allowed to warm to room temperature and stirred for 1 h, then it was cooled again to −78 °C. A solution of trimethyltin chloride 160 mg (2.3 equiv) in THF (4 mL) was added slowly to the reaction mixture, which was then brought back to room temperature and stirred overnight. The reaction mixture was quenched with water, extracted in dichloromethane, and washed several times with water. The organic layer was dried over $MgSO_4$, and the solvent was evaporated under reduced pressure to yield **15** (165 mg, 55 %). The product was used without further purification. ^{1}H NMR (200 MHz, $CDCl_3$, 25 °C): 0.30 (s, 18H; CH_3Sn), 0.87 (m, 6H; CH_3 alkyl chain), 1.19 (m, 20H; CH_2 alkyl chain), 1.59 (m, 4H; CH_2 alkyl chain), 2.71 (t, ^3J = 7.8 Hz, 4H; CH_2 thioph.), 6.93 (m, 4H; H_4), 7.02 (s, 2H; $H_{3'}$), 7.17 (s, 2H; H_4); EI-MS *m*/*z* (%): 881 (18) [M^+], 718 (51), 554 (100).

5,5‴-bis(vinyl)-3,3‴-bis(octyl)-2,2′:5′,2″:5″,2‴quaterthiophene (16): Dibromoquaterthiophene **15** (0.12 g, 0.168 mmol), vinyl trimethyltin (0.267 g, 0.84 mmol, 5 equiv), and $Pd(PPh_3)_4$ (9 mg, 7.8 mmol) were heated under argon in degassed DMF (5 mL) at 80 °C for 6 h. The crude reaction mixture was then quenched with water, extracted with dichloromethane, and dried over $MgSO_4$. The crude product was purified by column chromatography over neutral alumina eluted with petroleum ether to yield **16** (78 mg, 76 %). ^{1}H NMR (200 MHz, $CDCl_3$, 25 °C): 0.85 (t, ^3J = 5.8 Hz, 6H; CH_3 alkyl chain), 1.31 (m, 20H; CH_2 alkyl chain), 1.64 (m, 4H; CH_2 alkyl chain), 2.72 (t, ^3J = 6.8 Hz, 4H; CH_2 thioph.), 5.14 (d, ^3J = 10.8 Hz, 2H; H_3 vinyl), 5.56 (d, ^3J = 17.4 Hz, 2H; H_2 vinyl), 6.71 (dd, ^3J = 10.8 Hz, ^3J = 17.4 Hz, 2H; H_1 vinyl), 6.81 (s, 2H; H_4), 7.03 (d, ^3J = 3.7 Hz, 2H; $H_{4'}$), 7.17 (d, ^3J = 3.7 Hz, 2H; $H_{3'}$). EI-MS *m*/*z* (%): 608 (80) [M^+], 596 (100), 582 (100), 554 (20); elemental analysis calcd (%) for $C_{36}H_{46}S_4$: C 71.23, H 7.64, S 21.13, found: C 71.18, H 7.66, S 21.16.

5,5‴-bis(trimethylsilylethynyl)-3,3‴-bis(octyl)-2,2′:5′,2″:5″,2″-quaterthiophene (17): Dibromoquaterthiophene **14** (150 mg, 0.21 mmol), dry triethylamine (6 mL), $Pd_2(dba)_3 \cdot CHCl_3$.(2 mg, 1.6 mmol),$P(Ph)_3$ (16 mg, 61 mmol), and CuI (2 mg, 10 mmol) were added in a Schlenk tube. The reaction mixture was degassed with argon and stirred at room temperature for 15 minutes. Then trimethylsilylacetylene (103 mg, 1.03 mmol) and diisopropylamine (90 mL) were syringed into the reaction mixture that was heated at 70 °C overnight. The reaction mixture was poured into water and extracted with dichloromethane. The organic layer was washed with brine and dried over $MgSO_4$, and the solvents were removed by rotary evaporation. The resulting product was purified by column chromatography over silica gel eluted with petroleum ether to yield **17** (126 mg, 80 %). ^{1}H NMR (200 MHz, $CDCl_3$, 25 °C): 0.25 (s,18H; CH_3-Si), 0.87 (m, 6H; CH_3 alkyl chain), 1.31 (m, 20H; CH_2 alkyl chain), 1.64 (m, 4H; CH_2 alkyl chain), 2.75 (t, ^3J = 6.8 Hz, 4H; CH_2 thioph.), 7.03 (d, ^3J = 3.8 Hz, 2H; $H_{4'}$), 7.07 (s, 2H; H_4), 7.12 (d, ^3J = 3.8 Hz, 2H; $H_{3'}$); EI-MS *m*/*z* (%): 746 (100) [M^+], 648 (16), 515 (10); elemental analysis calcd (%) for $C_{42}H_{58}S_4Si_2$: C 67.50, H 7.82, S 17.16; found: C 67.82, H 7.52, S 17.34.

5,5‴-bis(ethynyl)-3,3‴-bis(octyl)-2,2′:5′,2″:5″,2‴quaterthiophene (18): Bis(trimethylsilylethynyl)quaterthiophene **17** (100 mg, 0.13 mmol) in benzene (5 mL) was mixed with a solution of KOH (4.8 mg, 0.8 equiv. in 1 mL methanol). The mixture was stirred at room temperature for 3 h. The reaction mixture was poured into water and extracted with benzene, dried over $MgSO_4$ and purified by column chromatography over neutral alumina eluted with petroleum ether to yield **18** (62 mg, 72 %). ^{1}H NMR (200 MHz, $CDCl_3$, 25 °C): 0.88 (m, 6H; CH_3 alkyl chain), 1.62 (m, 20H; CH_2 alkyl chain), 1.84 (m, 4H; CH_2 alkyl chain), 2.76 (t, ^3J = 7 Hz, 4H; CH_2 thioph.), 3.39 (s, 2H; H alkyne), 7.04 (d, ^3J = 3.8 Hz, 2H; $H_{4'}$), 7.11 (s, 2H; H_4), 7.12 (d, ^3J = 3.8 Hz, 2H; $H_{3'}$); EI-MS *m*/*z* (%): 666 (100) [M^+]; elemental analysis calcd (%) for $C_{36}H_{42}S_4$: C 71.71, H 7.02, S 21.27; found: C 71.87, H 7.33, S 21.43.

5,15-bis(3,5-di*tert*-butylphenyl)porphyrin (6): Freshly distilled dichloromethane (670 mL) in a round-bottomed flask protected from light and fitted with rubber septum was purged with bubbling argon for 1 h at room temperature. Then 3,5-di*tert*-butylbenzaldehyde (0.746 g, 3.42 mmol) and dipyrromethane (0.500 g, 3.42 mmol) were added. The stirring and bubbling with argon were continued for an additional 30 min, then trifluoroacetic acid (215 mL) was added by syringe in one portion. After this addition was complete, the reaction mixture changed immediately from colorless to yellow. The reaction mixture was then stirred for 15 h at room temperature and turned dark red after that time. A solution of 2,3-dichloro-5,6-dicyanobenzoquinone (DDQ, 1 g, 4.40 mmol) in toluene (25 mL) was then added by syringe in one go. The mixture was stirred for an additional 30 min. The solvent was evaporated to dryness in vacuum. The crude mixture was purified by flash chromatography on neutral alumina (petroleum ether/dichloromethane 80:20) to yield a purple-black powder (1.1 g, 73 %). ^{1}H NMR (200 MHz, $CDCl_3$, 25 °C): −2.99 (s, 2H; NH), 1.57 (s, 36H; *t*Bu), 7.85 (t, 2H, *J* = 1.8 Hz; phenyl H_p), 8.15 (d, 4H, ^3J = 1.8 Hz; phenyl H_o), 9.13 (d, ^3J = 4.7 Hz, 4H; β-pyrrolic H_2), 9.39 (d, ^3J = 4.7 Hz, 4H; β-pyrrolic H_3), 10.31 (s, 2H; H *meso*). ES$^+$-MS: *m*/*z*: calcd for $C_{48}H_{54}N_4$, 686.43; found 687.4 [M^++H].

5-bromo-10,20-bis(3,5-di*tert*-butylphenyl)porphyrin (7): 5,15-bis(3,5-di*tert*-butylphenyl)porphyrin (**6**) (300 mg, 0.435 mmol) was dissolved in dichloromethane (100 mL) and cooled to −40 °C. *N*-Bromosuccinimide (78 mg, 0.438 mmol) was added directly to the flask over 1 h, and the reaction was followed by TLC (dichloromethane/petroleum ether 15:85). After the reaction the reaction had reached completion, it was quenched with acetone/water (1:1, 20 mL). The solvents were evaporated, and the product was washed with several portions of dichloromethane and dried with $MgSO_4$. Porphyrin **7** was precipitated with petroleum ether and filtered off to yield a purple/black solid (216 mg, 65 %) contaminated with less than 10 % of dibromoporphyrin. An analytical sample of **7** was obtained by column chromatography over silica gel (petroleum ether/dichloromethane 80:20). ^{1}H NMR (400 MHz, $CDCl_3$, 25 °C): −2.91 (s, 2H; NH), 1.56 (s, 36H; *t*Bu), 7.84 (t, ^3J = 2.0 Hz, 2H; phenyl H_p), 8.08 (d, ^3J = 2.0 Hz, 4H; phenyl H_o), 8.99 (d, ^3J = 2.2 Hz, 2H; β-pyrrolic H_{13}), 9.02 (d, ^3J = 2.2 Hz, 2H; β-pyrrolic H_{12}), 9.29 (d, ^3J = 4.7 Hz, 2H; β-pyrrolic H_2), 9.75 (d, ^3J = 4.7 Hz, 2H; β-pyrrolic H_3), 10.16 (s, 1H; H *meso*); ES$^+$-MS: *m*/*z*: calcd for $C_{48}H_{53}BrN_4$, 764.35; found 765.4 [M^++H].

5,10,15-tris-(3,5-di*tert*-butylphenyl)porphyrin (8): A Schlenk tube was charged with 5-bromo-10,20-bis[3,5-di(*tert*-butyl)phenyl]porphyrin **7** (0.410 g, 0.53 mmol), 3,5-di(*tert*-butyl)phenylboronic acid (0.188 g, 0.80 mmol), $Ba(OH)_2 \cdot 8H_2O$ (0.254 g, 0.80 mmol), $Pd_2dba_3 \cdot CHCl_3$ (0.055 g, 0.053 mmol), PPh_3 (0.110 g, 0.42 mmol), DME (20 mL), and water (0.5 mL). The purple suspension was degassed by the freeze-pump-thaw method (three cycles), and the mixture was then heated at 100 °C under N_2 for 17 h. The reaction mixture was worked up by adding an equal volume of ether and washed with Na_2CO_3 saturated, with water, and finally with brine. The organic layer was dried over $MgSO_4$. The solvent was evaporated, and the crude product was purified by column chromatography on silica gel (petroleum ether/dichloromethane 90:10). The purple/red band was collected and evaporated to dryness to give a purple red solid (426 mg, 92 %). ^{1}H NMR (400 MHz, $CDCl_3$, 25 °C): −2.88 (s, 2H; NH), 1.51 (s, 18H; *t*Bu), 1.55 (s, 36H; *t*Bu), 7.81 (m, 3H; phenyl H_p), 8.08 (d, ^3J = 1.8 Hz, 2H; phenyl H_o), 8.12 (d, ^3J = 1.8 Hz, 4H; phenyl H_o), 8.92 (d, ^3J = 4.7 Hz, 2H; β-pyrrolic H_8), 9.06 (d, *J* = 4.7 Hz, 2H; β-pyrrolic H_2), 9.34 (d, ^3J = 4.7 Hz, 2H; β-pyrrolic H_3), 9.96 (d, ^3J = 4.7 Hz, 2H; β-pyrrolic H_2), 10.20 (s, 1H; H *meso*); ES$^+$-MS: *m*/*z*: calcd for $C_{62}H_{74}N_4$, 875.28; found 876.3 [M^++H].

5,5′-bis{zinc(II)-10,15,20-tris(3,5-di*tert*-butylphenyl)-5-porphyrinyl}-2,2′-bisthiophene (1ZZ): Zinc iodoporphyrin **10**[11] (90 mg 84.5 μmol), 5,5′-bis(trimethylstannyl)-2,2′-bisthiophene **12** (20 mg, 40.7 μmol), $Pd_2(dba)_3 \cdot CHCl_3$ (11 mg, 10 mmol), PPh_3 (22 mg, 84 mmol), and dry DMF (10 mL) were placed a Schlenk tube, and degassed for 15 minutes under ultrasound. The mixture was protected from light and heated at 90 °C for 15 h. The reaction mixture was poured into water and extracted with dichloromethane, and the organic layer was washed with water, dried over $MgSO_4$. The solvents were evaporated under vacuum and purified first by column chromatography and then by preparative TLC (petroleum ether/dichloromethane 7:3) to yield dyad **1ZZ** (62 mg, 72 %). ^{1}H NMR (400 MHz, $CDCl_3$, 25 °C): 1.50 (s, 36H; *t*Bu), 1.53 (s, 72H; *t*Bu), 7.78 (t, ^3J = 2 Hz, 2H; phenyl H_{p2}), 7.8 (t, ^3J = 2 Hz, 4H; phenyl H_{p1}), 7.81 (d, ^3J = 3.6 Hz, 2H; H_3), 7.92 (d, *J* = 3.6 Hz, 2H; H_4), 8.08 (d, ^3J = 2 Hz, 4H; phenyl H_{o2}), 8.17 (d, ^3J = 1.6 Hz, 8H; phenyl H_{o1}), 9.01 (s, 8H; β-pyrrolic H_{12}, H_{13}), 9.07 (d, ^3J = 4.8 Hz, 4H; β-pyrrolic H_2), 9.42 (d, ^3J = 4.8 Hz, 4H; β-pyrrolic H_3); UV/Vis (CH_2Cl_2): λ_{max} (ε) = 427 (650000), 553 (60000), 599 nm (32000); ES$^+$-MS: *m*/*z*: calcd for $C_{132}H_{146}N_8S_2Zn_2$, 2034.9695; found 2034.9762 [M^+].

5,5‴-bis[zinc(II)-10,15,20-tris(3,5-di*tert*-butylphenyl)-5-porphyrinyl]-3,3‴-bis(octyl)-2,2′:5′,2″:5″,2‴-quaterthiophene (2ZZ): A Schlenk tube was charged with zinc iodoporphyrin **10** (52 mg, 48.8 μmol), bis(trimethylstannyl)quaterthiophene **15** (20 mg, 22.7 μmol), $Pd_2(dba)_3 \cdot CHCl_3$ (5 mg, 4.7 mmol), PPh_3 (10 mg, 38 mmol), and dry DMF (10 mL) and degassed for 15 minutes under ultrasound. The mixture was protected from light and heated at 80 °C for 15 h. The reaction mixture was poured into water and extracted with dichloromethane, and the organic layer was washed with water and dried over $MgSO_4$. The solvents were evaporated under vacuum and purified by preparative TLC (petroleum ether/dichloromethane 7:3) to yield dyad **2ZZ** (36 mg, 60 %). ^{1}H NMR (400 MHz, $CDCl_3$, 25 °C): 1.53 (s, 36H; *t*Bu), 1.55 (s, 102H; alkyl chain), 3.18 (t, $^3J = 7.5$ Hz, 4H; CH_2 thioph.), 7.35 (AB system, $^3J = 4$ Hz, 4H; $H_{3'}$, $H_{4'}$), 7.79 (s, 2H; H_4), 7.80 (t, $^3J = 2$ Hz, 2H; phenyl H_{p2}), 7.81 (t, $^3J = 2$ Hz, 4H; phenyl H_{p1}), 8.09 (d, $^3J = 1.6$ Hz, 4H; phenyl H_{o2}), 8.11 (d, $^3J = 1.6$ Hz, 8H; phenyl H_{o1}), 9.01 (s, 8H; β-pyrrolic H_{12}, H_{13}), 9.05 (d, $^3J = 4.8$ Hz, 4H; β-pyrrolic H_2), 9.37 (d, $^3J = 4.8$ Hz, 4H; β-pyrrolic H_3); UV/Vis (CH_2Cl_2): λ_{max} (ε) = 424 (550000), 554 (51000), 595 (25000); ES$^+$-MS: *m*/*z*: calcd for $C_{156}H_{182}N_8S_4Zn_2$, 2423.1953; found 2423.1887 [M^+].

5,5‴-bis[zinc(II)-10,15,20-tris(3,5-di*tert*-butylphenyl)-5-vinylporphyrin]-3,3‴-bis(octyl)-2,2′:5′,2″:5″,2‴-quaterthiophene (3ZZ): Zinc iodoporphyrin **10** (188 mg, 177 μmol), bisvinyl quarterthiophene (48 mg, 82 μmol), $Pd(OAc)_2$ (2 mg, 9 mmol), potassium carbonate (118 mg, 820 mmol), tetrabutylammonium bromide (54 mg, 170 μmol), lithium chloride (10 mg, 0.24 mmol) and dry DMF (10 mL) were placed into a Schlenk tube. The mixture was degassed with argon and was heated in an oil bath at 85 °C for 40 h. The reaction mixture was poured into water and extracted with ether, and the combined organic layers were washed with water and brine, and dried over $MgSO_4$. The solvents were evaporated under vacuum, and the resulting solid was purified by preparative TLC (petroleum ether/dichloromethane 7:3) to yield dyad **3ZZ** (160 mg, 74 %). ^{1}H NMR (400 MHz, $CDCl_3$, 25 °C): 0.8–1.7 (s, 138H, *t*Bu; alkyl chain), 2.94 (t, $^3J = 7$ Hz, 4H; CH_2 thioph.), 7.25 (s, 2H; H_4), 7.29 (d, $^3J = 3.7$ Hz, 2H; $H_{4'}$), 7.35 (d, $^3J = 3.7$ Hz, 2H; $H_{3'}$), 7.49 (d, $^3J = 15.6$ Hz, 2H; H_2 vinyl), 7.8 (s, 2H; phenyl H_{p2}), 7.83 (s, 4H; phenyl H_{p1}), 8.07 (s, 4H; phenyl H_{o2}), 8.1 (s, 8H; phenyl H_{o1}), 8.98 (AB system, $^3J = 4$ Hz, 8H; β-pyrrolic H_{12}, H_{13}), 9.08 (d, $^3J = 4.4$ Hz, 4H; β-pyrrolic H_2), 9.6 (d, $^3J = 15.6$ Hz, 2H; H_1 vinyl), 9.68 (d, $^3J = 4.4$ Hz, 4H; β-pyrrolic H_3); UV/Vis (CH_2Cl_2): λ_{max} (ε) = 426 (420000), 559 (44000), 620 (58000). ES$^+$-MS: *m*/*z*: calcd for $C_{160}H_{186}N_8S_4Zn_2$, 2475.2266; found 2475.2217 [M^+].

5,5‴-bis[zinc(II)-10,15,20-tris(3,5-di*tert*-butylphenyl)-5-ethynylporphyrin]-3,3‴-bis(octyl)-2,2′:5′,2″:5″,2‴-quaterthiophene (4ZZ): A two-necked round-bottom flask was charged with iodoporphyrin **9** (150 mg, 141 μmol), bis(ethynyl)quarterthiophene **18** (40 mg, 66.3 μmol), toluene (20 mL), and triethyl amine (4 mL). The mixture was bubbled with argon for 15 min under ultrasound. $AsPh_3$ (20 mg, 66 μmol) and $Pd_2(dba)_3 \cdot CHCl_3$ (17 mg, 66 μmol) were added to the mixture, and argon bubbling was continued for another 10 min. The reaction mixture was then heated in an oil bath at 50 °C for 30 h. The solvents were evaporated under vacuum, and the product was purified by preparative TLC (petroleum ether/dichloromethane 7:3) to yield dyad **4ZZ** (96 mg, 56 %). ^{1}H NMR (400 MHz, $CDCl_3$, 25 °C): 1.51 (s, 36H; *t*Bu), 1.55 (s, 102H; alkyl chain), 2.97 (t, $^3J = 7.8$ Hz, 4H; CH_2 thioph.), 7.25 (d, $^3J = 3.8$ Hz, 2H; $H_{4'}$), 7.29 (d, $^3J = 3.8$ Hz, 2H; $H_{3'}$), 7.59 (s, 2H; H_4), 7.79 (t, $^3J = 1.8$ Hz, 2H; phenyl H_{p2}), 7.83 (t, $^3J = 1.8$ Hz, 4H; phenyl H_{p1}), 8.04 (d, $^3J = 1.8$ Hz, 4H; phenyl H_{o2}), 8.09 (d, $^3J = 1.8$ Hz, 8H; phenyl H_{o1}), 8.82 (AB system, $^3J = 4$ Hz, 8H; β-pyrrolic H_{12}, H_{13}), 9.06 (d, $^3J = 4.8$ Hz, 4H; β-pyrrolic H_2), 9.71 (d, $^3J = 4.8$ Hz, 4H; β-pyrrolic H_3); UV/Vis (CH_2Cl_2): λ_{max} (ε) = 437 (300000), 448 (300000), 574 (33000), 632 (81000). ES$^+$-MS: *m*/*z*: calcd for $C_{160}H_{182}N_8S_4Zn_2$, 2471.1953; found 2471.1887 [M^+].

5‴-[10,15,20-tris(3,5-di*tert*-butylphenyl)-5-ethynylporphyrin]-5-ethynyl-3,3‴-bis(octyl)-2,2′:5′,2″:5″,2‴-quaterthiophene (4Z): Exactly the same conditions were used as for **4ZZ**, except for equimolar amounts of iodoporphyrin **9** (70 mg, 66 μmol) and bis(ethynyl)quarterthiophene **18** (40 mg, 66.3 μmol). Compound **4Z** was purified by preparative TLC (petroleum ether/dichloromethane 7:3) to yield **4Z** (37 mg, 36 %). ^{1}H NMR (400 MHz, $CDCl_3$, 25 °C): 1.51 (s, 36H; *t*Bu), 1.55 (s, 102H; alkyl chain), 2.82 (t, $^3J = 7.8$ Hz, 4H; CH_2 thioph.), 2.94 (t, $^3J = 7.8$ Hz, 4H; CH_2 thioph.), 3.45 (s, 1H; H alkyne), 6.97 (d, $^3J = 3.8$ Hz, 1H; $H_{4''}$), 7.07 (d, $^3J = 3.6$ Hz, 1H; $H_{3'}$), 7.22 (m, 2H; $H_{4'}$ and $H_{3''}$), 7.34 (s, 1H; H_4), 7.79 (t, $^3J = 1.8$ Hz, 1H; phenyl H_{p2}), 7.83 (t, $^3J = 1.8$ Hz, 2H; phenyl H_{p1}), 8.04 (d, $^3J = 1.8$ Hz, 2H; phenyl H_{o2}), 8.09 (d, $^3J = 1.8$ Hz, 4H; phenyl H_{o1}), 8.97 (AB system, $^3J = 4$ Hz, 4H; β-pyrrolic H_{12}, H_{13}), 9.05 (d, $^3J = 4.8$ Hz, 2H; β-pyrrolic H_2), 9.80 (d, $^3J = 4.8$ Hz, 2H; β-pyrrolic H_3); UV/Vis (CH_2Cl_2): λ_{max} (ε) = 428 (306000), 450 (249000), 568 (20000), 631 (53000). ES$^+$-MS: *m*/*z*: calcd for $C_{99}H_{114}N_4S_4Zn$, 1550.7218; found 1550.7152 [M^+].

General procedure for demetalation of the dyads: The biszinc dyad (40 mg) was dissolved in dichloromethane (20 mL) and degassed under argon. One drop of conc. HCl (35 %) was added, and the mixture was stirred for 5 min at room temperature. This solution was then transferred to a separating funnel, washed with an aqueous carbonate solution and then with water, and the organic layer was dried over $MgSO_4$. The solvent was removed by rotary evaporation, and the resulting solid was pure, since almost no destruction of the porphyrin occurred during this step. An analytically pure sample was, however, obtained after chromatography in the next step.

5,5′-bis[10,15,20-tris(3,5-di*tert*-butylphenyl)-5-porphyrinyl]-2,2′-bisthiophene (1HH): ^{1}H NMR (400 MHz, $CDCl_3$, 25 °C): 1.7 (s, 36H; *t*Bu), 1.8 (s, 72H; *t*Bu), 7.79 (m, 6H; phenyl H_p), 7.95 (d, $^3J = 3.5$ Hz, 2H; H_4), 7.97 (d, $^3J = 3.52$ Hz, 2H; H_3), 8.08 (d, $^3J = 1.8$ Hz, 4H; phenyl H_{o2}), 8.12 (d, $^3J = 1.8$ Hz, 8H; phenyl H_{o1}), 8.9 (s, 8H; β-pyrrolic H_{12}, H_{13}), 8.89 (d, $^3J = 4.9$ Hz, 4H; β-pyrrolic H_2), 9.33 (d, $^3J = 4.9$ Hz, 4H; β-pyrrolic H_3); UV/Vis (CH_2Cl_2): λ_{max} (ε) = 422 (390000), 519 (25000), 558 (18000), 592 (18000), 651 (86000); ES$^+$-MS: *m*/*z*: calcd for $C_{132}H_{151}N_8S_2$, 1912.1503; found 1912.1434 [M^++H].

5,5‴-bis[10,15,20-tris(3,5-di*tert*-butylphenyl)-5-porphyrinyl]-3,3‴-bis(octyl)-2,2′:5′,2″:5″,2‴-quaterthiophene (2HH): ^{1}H NMR (400 MHz, $CDCl_3$, 25 °C): −2.59 (s, 4H; NH), 1.53 (s, 36H; *t*Bu), 0.9–2 (m, 102H; alkyl chain), 3.19 (t, $^3J = 7.5$ Hz, 4H; CH_2 thioph.), 7.36 (AB system, $^3J = 4$ Hz, 4H; $H_{3'}$, $H_{4'}$), 7.79 (s, 2H; H_4), 7.81 (t, $^3J = 2$ Hz, 2H; phenyl H_{p2}), 7.83 (t, $^3J = 2$ Hz, 4H; phenyl H_{p1}), 8.1 (d, $^3J = 1.6$ Hz, 4H; phenyl H_{o2}), 8.12 (d, $^3J = 1.6$ Hz, 8H; phenyl H_{o1}), 8.9 (AB system, $^3J = 4$ Hz, 8H; β-pyrrolic H_{12}, H_{13}), 8.95 (d, $^3J = 4.8$ Hz, 4H; β-pyrrolic H_2), 9.28 (d, $^3J = 4.8$ Hz, 4H; β-pyrrolic H_3); UV/Vis (CH_2Cl_2): λ_{max} (ε) = 424 (520000), 520 (34000), 560 (26000), 591 (13000), 652 (12000); ES$^+$-MS: *m*/*z*: calcd for $C_{156}H_{187}N_8S_4$, 2300.3762; found 2300.3799 [M^+].

5,5‴-bis[10,15,20-tris(3,5-di*tert*-butylphenyl)-5-vinyl-porphyrin]-3,3‴-bis-(octyl)-2,2′:5′,2″:5″,2‴-quaterthiophene (3HH): ^{1}H NMR (400 MHz, $CDCl_3$, 25 °C): −2.29 (s, 4H; NH), 0.8–2 (m, 138H; *t*Bu and alkyl chain), 2.98 (t, $^3J = 7$ Hz, 4H; CH_2 thioph.), 7.26 (s, 2H; H_4), 7.32 (d, $^3J = 3.7$ Hz, 2H; $H_{4'}$), 7.35 (d, $^3J = 3.7$ Hz, 2H; $H_{3'}$), 7.53 (d, $^3J = 15.6$ Hz, 2H; H_2 vinyl), 7.83 (t, $^3J = 1.6$ Hz, 2H; phenyl H_{p2}), 7.86 (t, $^3J = 1.6$ Hz, 4H; phenyl H_{p1}), 8.11 (d, $J = 2$ Hz, 4H; phenyl H_{o2}), 8.15 (d, $^3J = 2$ Hz, 8H; phenyl H_{o1}), 8.9 (AB system, $^3J = 4$ Hz, 8H; β-pyrrolic H_{12}, H_{13}), 9. (d, $^3J = 4.8$ Hz, 4H; β-pyrrolic H_2), 9.55 (d, $^3J = 15.6$ Hz, 2H; H_1 vinyl), 9.58 (d, $^3J = 4.8$ Hz, 4H; β-pyrrolic H_3); UV/Vis (CH_2Cl_2): λ_{max} (ε) = 426 (310000), 589 (52000), 675 (26000); ES$^+$-MS: *m*/*z*: calcd for $C_{160}H_{190}N_8S_4$, 2351.3995; found 2351.3982 [M^+].

5,5‴-bis[10,15,20-tris(3,5-di*tert*-butylphenyl)-5-ethynylporphyrin]-3,3‴-bis-(octyl)-2,2′:5′,2″:5″,2‴-quaterthiophene (4HH): ^{1}H NMR (400 MHz, $CDCl_3$, 25 °C): −2.17 (s, 4H; NH), 0.8–2 (m, 36H, *t*Bu, 102H; alkyl chain), 2.95 (t, $^3J = 7.9$ Hz, 4H; CH_2 thioph.), 7.24 (d, $^3J = 4$ Hz, 2H; $H_{4'}$), 7.3 (d, $^3J = 4$ Hz, 2H; $H_{3'}$), 7.62 (s, 2H; H_4), 7.88 (t, $^3J = 1.6$ Hz, 2H; phenyl H_{p2}), 7.91 (t, $^3J = 1.6$ Hz, 4H; phenyl H_{p1}), 8.1 (d, $^3J = 1.6$ Hz, 4H; phenyl H_{o2}), 8.14 (d, $^3J = 1.6$ Hz, 8H; phenyl H_{o1}), 8.86 (AB system, $^3J = 4$ Hz, 8H; β-pyrrolic H_{12}, H_{13}), 9 (d, $^3J = 4.8$ Hz, 4H; β-pyrrolic H_2), 9.76 (d, $^3J = 4.8$ Hz, 4H; β-pyrrolic H_3); UV/Vis (CH_2Cl_2): λ_{max} (ε) = 442 (280000), 597 (65000), 681 (38000); ES$^+$-MS: *m*/*z*: calcd for $C_{160}H_{187}N_8S_4$, 2348.3762; found 2348.3843 [M^++H].

General procedure for zinc mono-metalation of the dyads: Bis-free-base dyad HH (30 mg) was dissolved in the mixture chloroform/methanol (6:4, 10 mL) mixture and the mixture was degassed. A solution of zinc acetate (5 mg in 1 mL of methanol) was injected dropwise and the reaction was continuously monitored by TLC. The addition was stopped when most of the free-base starting material had disappeared. The reaction yielded to a mixture of three porphyrins that were purified by preparative silica TLC eluted with hexane/dichloromethane (7:3).

5-[zinc(II)-10,15,20-tris(3,5-di*tert*-butylphenyl)-5-porphyrinyl]-5′-[10,15,20-tris(3,5-di*tert*-butylphenyl)-5-porphyrinyl]-2,2′-bisthiophene (1ZH): ^{1}H NMR (400 MHz, $CDCl_3$, 25 °C): −2.67 (s, 2H; NH), 1.49 (s, 36H; *t*Bu), 1.52 (s, 72H; *t*Bu), 7.8–7.85 (m, 6H; phenyl H_p), 7.91 (d, $^3J = 3.8$ Hz,

0947-6539/02/0813-3044 $ 20.00+.50/0 *Chem. Eur. J.* **2002**, *8*, No. 13

2H; H_3), 7.92 (d, $^3J = 3.8$ Hz, 2H; H_4), 8.05 (d, $^3J = 1.55$ Hz, 4H; phenyl H_{o2}), 8.1 (d, $^3J = 1.56$ Hz, 8H; phenyl H_{o1}), 8.8 (AB system, $^3J = 4$ Hz, 4H; β-pyrrolic H_{12H}, H_{13H}), 8.95 (AB system, $^3J = 4$ Hz, 4H; β-pyrrolic H_{12Zn}, H_{13Zn}), 8.95 (d, $^3J = 5$ Hz, 2H; β-pyrrolic H_{2H}), 9.04 (d, $^3J = 4.8$ Hz, 2H; β-pyrrolic H_{2Zn}), 9.3 (d, $^3J = 5$ Hz, 2H; β-pyrrolic H_{3H}), 9.8 (d, $^3J = 4.8$ Hz, 2H; β-pyrrolic H_{3Zn}); UV/Vis (CH_2Cl_2): λ_{max} (ε) = 426 (670000), 519 (29000), 556 (44000), 596 (21000), 651 (9000); ES$^+$-MS: *m*/*z*: calcd for $C_{132}H_{119}N_8S_2Zn$, 1974.0638; found 2423.1887 [M^++H].

5-[zinc(II)-10,15,20-tris(3,5-di*tert*-butylphenyl)-5-porphyrinyl]-5‴-[10,15,20-tris(3,5-di*tert*-butylphenyl)-5-porphyrinyl]-3,3‴-bis(octyl)-2,2′:5′,2″:5″,2‴-quaterthiophene (2ZH): ^{1}H NMR (400 MHz, $CDCl_3$, 25 °C): −2.6 (s, 2H; NH), 0.8–2 (m, 36H; *t*Bu, 102H; alkyl chain), 3.18 (t, $^3J = 8$ Hz, 4H; CH_2 thioph.), 7.35 (AB system, $^3J = 4$ Hz, 4H; $H_{3'}$, $H_{4'}$, $H_{3''}$, $H_{4''}$), 7.79 (s, 2H; H_4, $H_{4'''}$), 7.8–7.82 (m, 6H; phenyl H_p), 8.08 to 8.11 (m, 12H; phenyl H_o), 8.89 (s, 4H; β-pyrrolic H_{12H}, H_{13H}), 8.93 (d, $^3J = 4.8$ Hz, 2H; β-pyrrolic H_{2H}), 9.00 (AB system, $J = 4$ Hz, 4H; β-pyrrolic H_{12Zn}-H_{13Zn}), 9.05 (d, $^3J = 4.4$ Hz, 2H; β-pyrrolic H_{2Zn}), 9.26 (d, $^3J = 4.8$ Hz, 2H; β-pyrrolic H_{3H}), 9.36 (d, $^3J = 4.8$ Hz, 2H; β-pyrrolic H_{3Zn}); UV/Vis (CH_2Cl_2): λ_{max} (ε) = 425 (560000), 520 (22000), 556 (33000), 596 (16000), 652 (6 400); ES$^+$-MS: *m*/*z*: calcd for $C_{156}H_{185}N_8S_4Zn$, 2362.2897; found 2362.2795 [M^+].

5-[zinc(II)-10,15,20-tris(3,5-di*tert*-butylphenyl)-5-vinylporphyrin]-5‴-[10,15,20-tris(3,5-di*tert*-butylphenyl)-5-vinylporphyrin]-3,3‴-bis(octyl)-2,2′:5′,2″:5″,2‴-quaterthiophene (3ZH): ^{1}H NMR (400 MHz, $CDCl_3$, 25 °C): −2.37 (s, 2H; NH), 0.8–1.85 (m, 138H, *t*Bu; alkyl chain), 2.97 (t, $^3J = 6.5$ Hz, 4H; CH_2 thioph.), 7.17–7.35 (m, 6H; $H_{3'}$, $H_{4'}$, $H_{3''}$, $H_{4''}$, H_4, $H_{4'''}$), 7.52 (d, $^3J = 16$ Hz, 1H; H_{2H} vinyl), 7.54 (d, $^3J = 16$ Hz, 1H; H_{2Zn} vinyl), 7.87 (m, 2H; phenyl H_{p2}), 7.9 (m, 4H; phenyl H_{p1}), 8.11 (m, 4H; phenyl H_{o2}), 8.14 (m, 8H; phenyl H_{o1}), 8.87 (s, 4H; β-pyrrolic H_{12H}, H_{13H}), 8.98 (m, 6H; β-pyrrolic-H_{12Zn}, H_{13Zn} and β-pyrrolic H_{2H}), 9.09 (d, $^3J = 4.9$ Hz, 2H; β-pyrrolic H_{2Zn}), 9.55 (d, $^3J = 16$ Hz, 1H; H_{1H} vinyl), 9.6 (d, $^3J = 4.8$ Hz, 2H; β-pyrrolic H_{3H}), 9.65 (d, $^3J = 16$ Hz, 1H; H_{1Zn} vinyl), 9.72 (d, $^3J = 4.8$ Hz, 2H; β-pyrrolic H_{3Zn}); UV/Vis (CH_2Cl_2): λ_{max} (ε) = 427 (270000), 575 (28000), 609 (39000), 668 (13000); ES$^+$-MS: *m*/*z*: calcd for $C_{160}H_{188}N_8S_4Zn$, 2413.3132; found 2413.3145 [M^+].

5-[zinc(II)-10,15,20-tris(3,5-di*tert*-butylphenyl)-5-ethynylporphyrin]-5‴-[10,15,20-tris(3,5-di*tert*-butylphenyl)-5-ethynylporphyrin]-3,3‴-bis(octyl)-2,2′:5′,2″:5″,2‴-quaterthiophene (4ZH): ^{1}H NMR (400 MHz, $CDCl_3$, 25 °C): −2.17 (s, 2H; NH), 0.8–1.8 (m, 36H; *t*Bu, 102 H and alkyl chain), 2.94 (t, $^3J = 8$ Hz, 4H; CH_2 thioph.), 7.22–7.26 (series of doublets, 4H; $H_{3'}$, $H_{4'}$, $H_{3''}$, $H_{4''}$), 7.55 (s, 1H; $H_{4'''}$), 7.56 (s, H; H_4), 7.7 (m, 2H; phenyl H_{p2}), 7.8 (s, 4H; phenyl H_{p1}), 8.01 (d, $^3J = 1.6$ Hz, 2H; phenyl H_{o2H}), 8.02 (d, $^3J = 1.6$ Hz, 2H; phenyl H_{o2Zn}), 8.06 (d, $^3J = 1.6$ Hz, 4H; phenyl H_{o1H}), 8.07 (dd, $^3J = 1.6$ Hz, 4H; phenyl H_{o1Zn}), 8.80 (AB system, $^3J = 5$Hz, 4H; β-pyrrolic H_{12H}, H_{13H}), 8.91 (AB system, $^3J = 4.8$ Hz, 4H; β-pyrrolic H_{12Zn}, H_{13Zn}), 8.94 (d, $^3J = 4.8$ Hz, 2H; β-pyrrolic H_{2H}), 9.05 (d, $^3J = 4.4$ Hz, 2H; β-pyrrolic H_{2Zn}), 9.68 (d, $^3J = 4.8$ Hz, 2H; β-pyrrolic H_{3H}), 9.78 (d, $^3J = 4.4$ Hz, 2H; β-pyrrolic H_{3Zn}); UV/Vis (CH_2Cl_2): λ_{max} (ε) = 444 (305000), 596 (45000), 630 (51000), 680 (22 700); ES$^+$-MS: *m*/*z* (%): calcd for $C_{160}H_{185}N_8S_4Zn$, 2410.2897; found 2410.2930 [M^+].

Acknowledgements

This work was financially supported by CNRS. The authors express their gratitude to Dr. M. Hissler and Dr. G. Simmoneaux (Rennes University) for fluorimetry and we thank Stephane Guillerez (CEA, Grenoble) for experimental advice for the preparation of 3,3‴-bis(octyl)-5,5‴-bis(trimethylstannyl)-2,2′:5′,2″:5″,2‴quaterthiophene. L. H. acknowledges financial support from the Swedish Foundation for Strategic Research and the Knut and Alice Wallenberg Foundation.

[1] V. Balzani, F. Scandola, *Supramolecular Photochemistry*, Ellis Horwood, Chischester, UK, **1991**.
[2] V. Balzani, F. Scandola, *Compr. Supramol. Chem.* **1996**, *10*, 687.
[3] *Molecular Electronics* (Eds.: J. Jortner, M. Ratner), Blackwell Science, London, **1997**.
[4] a) C. Joachim, J. K. Gimzewski, A. Aviram, *Nature* **2000**, *408*, 541; b) Y. Shirota, *J. Mater. Chem.* **2000**, *10*, 1.
[5] a) G. C. Allen, N. S. Hush, *Prog. Inorg. Chem.* **1967**, *8*, 357; b) C. Joachim, *Chem. Phys.* **1987**, *116*, 339; c) S. Larsson, *Chem. Phys. Lett.* **1982**, *90*, 136.
[6] a) R. A. Marcus, *J. Chem. Phys.* **1976**, *24*, 966; b) R. A. Marcus, N. Sutin, *Springer Ser. Chem. Phys.* **1985**, *42*, 226; c) R. A. Marcus, N. Sutin, *Biochim. Biophys. Acta* **1985**, *811*, 265; d) M. Bixon, J. Jortner, *Adv. Chem. Phys.* **1999**, *106*, 35.
[7] W. B. Davis, W. A. Svec, M. A. Ratner, M. R. Wasielewski, *Nature* **1998**, *396*, 60.
[8] D. Segal, A. Nitzan, W. B. Davis, M. R. Wasielewski, M. A. Ratner, *J. Phys. Chem. B* **2000**, *104*, 3817.
[9] a) D. N. Beratan, *J. Am. Chem. Soc* **1986**, *108*, 4321; b) M. N. Paddon-Row, J. W. Verhoeven, *New J. Chem.* **1991**, *15*, 107; c) G. L. Closs, J. R. Miller, *Science* **1988**, *240*, 440.
[10] V. L. Davidson, *Acc. Chem. Res.* **2000**, *33*, 87.
[11] J. L. Sessler, B. Wang, S. L. Springs, C. T. Brown, *Compr. Supramol. Chem.* **1996**, *4*, 311.
[12] J. L. Sessler, M. R. Johnson, T. Y. Lin, S. E. Creager, *J. Am. Chem. Soc.* **1988**, *110*, 3659.
[13] Y.-Z. Hu, S. Tsukiji, S. Oishi, I. Hamachi, *J. Am. Chem. Soc* **2000**, *122*, 241.
[14] a) T. N. Putterits, V. Sundström, *Acc. Chem. Res.* **1996**, *29*, 381; b) A. Damjanovic, T. Ritz, K. Schulten, *Int. J. Quantum Chem.* **2000**, *77*, 139; c) A. Zoumi, *Photosynthesis: Mechanisms and Effects*, Kluwer, Dordrecht, **1998**.
[15] K. A. Jolliffe, T. D. M. Bell, K. P. Ghiggino, S. J. Langford, M. N. Paddon-Row, *Angew. Chem.* **1998**, *110*, 959; *Angew. Chem. Int. Ed.* **1998**, *37*, 916.
[16] K. A. Jolliffe, S. J. Langford, A. M. Oliver, M. J. Shephard, M. N. Paddon-Row, *Chem. Eur. J.* **1999**, *5*, 2518.
[17] a) D. Gust, T. A. Moore, A. L. Moore, J. A. A. Krasnovsky, P. A. Lindell, D. Nicodem, J. DeGraziano, P. McKerrigan, L. R. Makings, P. J. Pessiki, *J. Am. Chem. Soc.* **1993**, *115*, 5684; b) D. Gust, T. A. Moore, A. L. Moore, S. J. Lee, E. Bittersmann, D. K. L. Luttrul, A. A. Rehms, J. DeGraziano, X. C. Ma, F. Gao, R. E. Belford, T. T. Trier, *Science* **1990**, *248*, 199; c) D. Kuciauskas, P. A. Lindell, S. Lin, T. E. Johnson, S. J. Weghorn, J. S. Lindsey, A. L. Moore, T. A. Moore, D. Gust, *J. Am. Chem. Soc.* **1999**, *121*, 8604; d) D. Gust, T. A. Moore, A. L. Moore, F. Gao, D. K. Luttrull, J. M. DeGraziano, X. C. Ma, L. R. Makings, S. J. Lee, T. T. Trier, E. Bittersmann, G. R. Seely, S. Woodward, R. V. Benasson, M. Rougee, F. C. De Schryver, M. Van der Auweraer, *J. Am. Chem. Soc.* **1991**, *113*, 3638.
[18] a) J. P. Collin, P.Gavina, V. Heitz, J. P. Sauvage, *Eur. J. Inorg. Chem.* **1998**, *1*, 1; b) M. Andersson, M. Linke, J.-C. Chambron, J. Davidsson, V. Heitz, J.-P. Sauvage, L. Hammarström, *J. Am. Chem. Soc.* **2000**, *122*, 3526; c) M.-J. Blanco, M. Consuelo Jimenez, J.-C. Chambron, V. Heitz, M. Linke, J.-P. Sauvage, *Chem. Soc. Rev.* **1999**, *28*, 293; d) J.-C. Chambron, J.-P. Collin, J.-O. Dalbavie, C. O. Dietrich-Buchecker, V. Heitz, F. Odobel, N. Solladie, J.-P. Sauvage, *Coord. Chem. Rev.* **1998**, *178–180*, 1299; e) M. Linke, J.-C. Chambron, V. Heitz, J.-P. Sauvage, S. Encinas, F. Barigelletti, L. Flamigni, *J. Am. Chem. Soc.* **2000**, *122*, 11834; f) J.-P. Sauvage, *Science* **2001**, *291*, 2105.
[19] a) A. Osuka, S. Nakajima, K. Maruyama, N. Mataga, T. Asahi, I. Yamazaki, Y. Nishimura, T. Ohno, K. Nozaki, *J. Am. Chem. Soc.* **1993**, *115*, 4577; b) M. Ohkohchi, A. Takahashi, N. Mataga, T. N. Okada, A. Osuka, H. Yamada, K. Maruyama, *J. Am. Chem. Soc.* **1993**, *115*, 12137; c) T. Nagata, A. Osuka, K. Maruyama, *J. Am. Chem. Soc.* **1990**, *112*, 3054; d) A. Osuka, K. Maruyama, N. Mataga, T. Asahi, I. Yamazaki, N. Tamai, *J. Am. Chem. Soc.* **1990**, *112*, 4958; e) A. Osuka, N. Tanabe, S. Kawabata, I. Yamazaki, Y. Nishimura, *J. Org. Chem.* **1995**, *60*, 7177; f) T. Asahi, M. Ohkohchi, R. Matsusaka, N. Mataga, R. P. Zhang, A. Osuka, K. Maruyama, *J. Am. Chem. Soc.* **1993**, *115*, 5665.
[20] a) V. S. Y. Lin, M. J. Therien, *Chem. Eur. J.* **1995**, *1*, 645; b) V. S. Y. Lin, S. G. DiMagno, M. J. Therien, *Science* **1994**, *264*, 1105.
[21] S. M. Lecours, S. G. DiMagno, M. J. Therien, *J. Am. Chem. Soc* **1996**, *118*, 11854.
[22] H. Oevering, M. N. Paddon-Row, M. Heppener, A. M. Oliver, E. Cotsaris, J. W. Verhoeven, N. S. Hush, *J. Am. Chem. Soc.* **1987**, *109*, 3258.
[23] W. B. Davis, M. A. Ratner, M. R. Wasielewski, *J. Am. Chem. Soc.* **2001**, *123*, 7877.

[24] a) K. Kilsa, J. Kajanus, A. N. Macpherson, J. Martensson, B. Albinsson, *J. Am. Chem. Soc.* **2001**, *123*, 3069; b) K. Kilsa, A. N. Macpherson, T. Gillbro, J. Martensson, B. Albinsson, *Spectrochim. Acta Part A* **2001**, *57A*, 2213; c) K. Kilsa, J. Kajanus, S. Larsson, A. N. Macpherson, J. Martensson, B. Albinsson, *Chem. Eur. J.* **2001**, *7*, 2122.
[25] a) H. S. Cho, D. H. Jeong, M.-C. Yoon, Y. H. Kim, Y. R. Kim, D. Kim, S. C. Jeoung, S. K. Kim, N. Aratani, H. Shinmori, A. Osuka, *J. Phys. Chem. A* **2001**, *105*, 4200; b) D. L. Dexter, *J. Chem. Phys.* **1953**, *21*, 836; c) K. K. Jensen, S. B. van Berlekom, J. Kajanus, J. Maartensson, B. Albinsson, *J. Phys. Chem. A* **1997**, *101*, 2218; d) K. Kilsa, J. Kajanus, J. Martensson, B. Albinsson, *J. Phys. Chem. B* **1999**, *103*, 7329.
[26] D. Dolphin, *The Porphyrins*, *Vols. 1–6*, Harcourt Brace Jovanovich, New York, **1978**.
[27] K. Kalyanasundaram, *Photochemistry of Polypyridine and Porphyrin Complexes*, Academic Press, London, **1992**.
[28] M. R. Wasielewski, *Chem. Rev.* **1992**, *92*, 435.
[29] K. M. Kadish, N. Guo, E. van Caemelbecke, A. Froiio, R. Paolesse, D. Monti, P. Tagliatesta, T. Boschi, L. Prodi, F. Bolletta, N. Zaccheroni, *Inorg. Chem.* **1998**, *37*, 2358.
[30] K. M. Kadish, K. M. Smith, R. Guilard, *The Porphyrin Handbook*, *Vol. 10*, Academic Press, San Diego, **2000**.
[31] a) D. P. Arnold, G. A. Heath, *J. Am. Chem. Soc.* **1993**, *115*, 12197; b) D. P. Arnold, L. J. Nitschinsk, *Tetrahedron* **1992**, *48*, 8781; c) D. P. Arnold, D. A. James, C. H. L. Kennard, G. Smith, *Chem. Commun.* **1994**, 2131; d) R. Stranger, J. E. McGrady, D. P. Arnold, I. Lane, G. A. Heath, *Inorg. Chem.* **1996**, *35*, 7791.
[32] a) P. N. Taylor, A. P. Wylie, J. Huuskonen, H. L. Anderson, *Angew. Chem.* **1998**, *110*, 1033; *Angew. Chem. Int. Ed.* **1998**, *37*, 916; b) H. L. Anderson, *Chem. Commun.* **1999**, 2323.
[33] a) J. J. Gosper, M. Ali, *Chem. Commun.* **1994**, 1707; b) D. A. Schultz, H. Lee, R. K. Kumar, K. P. Gwaltney, *J. Org. Chem.* **1999**, *64*, 9124; c) J. Wykto, V. Berl, M. McLaughlin, R. R. Tykwinski, M. Schreiber, F. Diederich, C. Boudon, J. P. Gisselbrecht, M. Gross, *Helv. Chim. Acta* **1998**, *81*, 1964; d) M. G. H. Vicente, L. Jaquinod, K. Smith, *Chem. Commun.* **1999**, 1771.
[34] a) P. F. H. Schwab, M. D. Levin, J. Michl, *Chem. Rev.* **1999**, *99*, 1863; b) R. E. Martin, F. Diederich, *Angew. Chem.* **1999**, *111*, 1440; *Angew. Chem. Int. Ed.* **1999**, *38*, 1350.
[35] a) P. Bauerl, *Adv. Mater.* **1992**, *4*, 102; b) H. S. Nalva, *Handbook of Organic Conductive Molecules and Polymers*, *Vols. 1–4*, Wiley, Chichester, **1997**.
[36] a) J. Roncali, *Chem. Rev.* **1997**, *97*, 173; b) J. M. Tour, *Chem. Rev.* **1996**, *96*, 537.
[37] D. P. Arnold, D. A. James, *J. Org. Chem.* **1997**, *62*, 3460.
[38] a) F. Würthner, M. S. Vollmer, F. Effenberger, P. Emele, D. U. Meyer, H. Port, H. C. Wolf, *J. Am. Chem. Soc.* **1995**, 8090; b) M. S. Vollmer, F. Effenberger, T. Stümpfig, A. Hartschuh, H. Port, H. C. Wolf, *J. Org. Chem.* **1998**, *63*, 5080; c) M. S. Vollmer, F. Würthner, F. Effenberger, P. Emele, D. U. Meyer, T. Stümpfig, H. Port, H. C. Wolf, *Chem. Eur. J.* **1998**, *4*, 260.
[39] H. Higuchi, T. Ishikura, K. Miyabiyashi, M. Miyake, K. Yamamoto, *Tetrahedron Lett.* **1999**, *40*, 9091.
[40] a) J. Rodriguez, C. Kirmaier, M. R. Johnson, R. A. Friesner, D. Holten, J. L. Sessler, *J. Am. Chem. Soc.* **1991**, *113*, 1652; b) S. Shanmugathasan, C. Edwards, R. W. Boyle, *Tetrahedron* **2000**, *56*, 1025.
[41] a) X. Zhou, K. S. Chan, *J. Org. Chem.* **1998**, *63*, 99; b) X. Zhou, M. K. Tse, T. S. M. Wan, K. S. Chan, *J. Org. Chem.* **1996**, *61*, 3590; c) S. G. Dimagno, V. S. Y. Lin, M. J. Therien, *J. Org. Chem.* **1993**, *58*, 5983; d) S. G. Dimagno, V. S. Y. Lin, M. J. Therien, *J. Am. Chem. Soc.* **1993**, *115*, 2513.
[42] a) M. Ravikanth, J. P. Strachan, F. Li, J. S. Lindsey, *Tetrahedron* **1998**, *54*, 7721; b) R. W. Wagner, T. E. Johnson, J. S. Lindsey, *J. Am. Chem. Soc.* **1996**, *118*, 11166; c) J. P. Strachan, S. Gentemann, J. Seth, W. A. Kalsbeck, J. S. Lindsey, D. Holten, D. F. Bocian, *Inorg. Chem.* **1998**, *37*, 1191.
[43] F. Odobel, F. Suzenet, E. Blart, J.-P. Quintard, *Org. Lett.* **2000**, *1*, 131.
[44] A. Nakano, H. Shimidzu, A. Osuka, *Tetrahedron Lett.* **1998**, *39*, 9489.
[45] H. Nakanishi, N. Sumi, Y. Aso, T. Otsubo, *J. Org. Chem.* **1998**, *63*, 8632.
[46] a) F. Diederich, P. J. Stang, *Metal-Catalyzed Cross-Coupling Reactions*, Wiley, Weinheim, **1997**; b) S. P. Stanforth, *Tetrahedron* **1998**, *54*, 263.
[47] S. Mikami, K.-i. Sugiura, Y. Sakata, *Chem. Lett.* **1997**, 833.
[48] A. G. Hyslop, M. A. Kellett, P. M. Iovine, M. J. Therien, *J. Am. Chem. Soc.* **1998**, *120*, 12676.
[49] R. W. Boyle, C. K. Johnson, D. Dolphin, *Chem. Commun.* **1995**, 527.
[50] a) G. Barbarella, M. Zambianchi, L. Antolini, P. Ostoja, P. Maccagnani, A. Bongini, E. A. Marseglia, E. Tedesco, G. Gigli, R. Cingolani, *J. Am. Chem. Soc.* **1999**, *121*, 8920; b) J. Bras, S. Guillerez, B. Pepin-Donat, *Chem. Mater.* **2000**, *12*, 2372; c) G. A. Tolstikov, M. S. Miftakhov, N. A. Danilova, Y. L. Vel'der, L. V. Spirkhin, *Synthesis* **1989**, 633.
[51] a) R. F. Heck, J. P. Nolley, *J. Org. Chem.* **1972**, *37*, 2320; b) R. F. Heck, B. M. Trost, I. Flemming, *Comprehensive Organic Synthesis*, *Vol. 4*, Oxford, New York, **1991**; c) W. Cabri, I. Candiani, *Acc. Chem. Res.* **1995**, *28*, 2; d) I. P. Beletskaya, A. V. Cheprakov, *Chem. Rev.* **2000**, *100*, 3009.
[52] a) T. Jeffery, *Chem. Commun.* **1984**, 1287; b) R. Gauler, N. Risch, *Eur. J. Org. Chem.* **1998**, 1193; c) N. Risch, R. Gauler, R. Keuper, *Tetrahedron Lett.* **1999**, *40*, 2925; d) N. Risch, R. Gauler, *Tetrahedron Lett.* **1997**, *38*, 223.
[53] R. W. Wagner, T. E. Johnson, F. Li, J. S. Lindsey, *J. Org. Chem.* **1995**, *60*, 5266.
[54] a) J. J. Piet, P. N. Taylor, H. L. Anderson, A. Osuka, J. M. Warman, *J. Am. Chem. Soc.* **2000**, *122*, 1749; b) J. J. Piet, P. N. Taylor, B. R. Wegewijs, H. L. Anderson, A. Osuka, J. M. Warman, *J. Phys. Chem. B* **2001**, *105*, 97.
[55] Y. H. Kim, D. H. Jeong, D. Kim, S. C. Jeoung, H. S. Cho, S. K. Kim, N. Aratani, A. Osuka, *J. Am. Chem. Soc.* **2001**, *123*, 76.
[56] P. J. Spellane, M. Gouterman, A. Antipas, S. Kim, Y. C. Liu, *Inorg. Chem.* **1980**, *19*, 386.
[57] a) D. T. Hermann, A. C. Schindler, K. Polborn, R. Gompper, S. Stark, A. Parusel, G. Grabner, G. Köhler, *Chem. Eur. J.* **1999**, *5*, 3208; b) A. Parusel, *J. Mol. Model.* **1998**, *4*, 366.
[58] M. Gouterman, *Optical Spectra and Electronic Structure of Porphyrins and Related Rings*, *Vol. 3*, Academic Press, New York, **1978**.
[59] This is confirmed by the fluorescence lifetime results that gave a correspondingly small fraction of an unquenched lifetime (ca. 2 ns) in the spectral region of the zinc porphyrin emission. The impurity is a degradation product created during transportation of the compounds for photophysical measurements, as shown by the concomitant appearance of new spots on TLC plates for these samples.
[60] T. Förster, *Discuss. Faraday Soc.* **1959**, *27*, 7.
[61] a) J. P. Strachan, S. Gentemann, J. Seth, W. A. Kalsbeck, J. S. Lindsey, D. Holten, D. F. Bocian, *Inorg. Chem.* **1998**, *37*, 1191; b) R. K. Lammi, A. Ambroise, T. Balasubramanian, R. W. Wagner, D. F. Bocian, D. Holten, J. S. Lindsey, *J. Am. Chem. Soc.* **2000**, *122*, 7579.
[62] C. van Pham, H. B. Mark, H. Zimmer, *Synth. Comm.* **1986**, *16*, 689.
[63] L. L. Miller, Y. Yu, *J. Org. Chem.* **1995**, *60*, 6813.
[64] M. S. Newman, L. F. Lee, *J. Org. Chem.* **1972**, *37*, 4468.
[65] T. H. Kawazura, Y. Ishii, *J. Organomet. Chem.* **1974**, *65*, 253.
[66] a) M. J. S. Dewar, E. G. Zoebisch, E. F. Healy, J. J. P. Stewart, *J. Am. Chem. Soc.* **1985**, *107*, 3902; b) M. J. S. Dewar, K. M. Merz, *Organometallics* **1988**, *7*, 522; c) M. J. S. Dewar, Y. C. Yuan, *Inorg. Chem.* **1990**, *29*, 3881.
[67] Spartan, version 4.0, Wavefunction, Inc., Irvine, CA, USA.
[68] HyperChem 5.1, HyperCube, Inc., FL, USA.
[69] A. J. Golder, K. B. Nolan, D. C. Povey, L. R. Milgrom, *Acta Crystallogr. C* **1988**, *44*, 1916.

Received: December 21, 2001 [F3758]

  0947-6539/02/0813-3046 $ 20.00+.50/0